The Company of Biologists

RESEARCH ARTICLE

Ionoregulatory aspects of the hypoxia-induced osmorespiratory compromise in the euryhaline Atlantic killifish (*Fundulus heteroclitus*): the effects of salinity

Marina Giacomin[1,*], John O. Onukwufor[1,2], Patricia M. Schulte[1] and Chris M. Wood[1,3]

ABSTRACT

The osmorespiratory compromise is a physiological trade-off between the characteristics of the gill that promote respiratory gas exchange and those that limit passive flux of ions and water with the environment. In hypoxia, changes in gill blood flow patterns and functional surface area that increase gas transfer can promote an exacerbation in ion and water flux. Our goal was to determine whether the osmorespiratory compromise is flexible, depending on environmental salinity (fresh, isosmotic and sea water) and oxygen levels (hypoxia) in euryhaline killifish, *Fundulus heteroclitus*. Plasma ion concentrations were minimally affected by hypoxia, indicating a maintenance of osmoregulatory homeostasis. In freshwater killifish, hypoxia exposure reduced branchial Na^+/K^+-ATPase and NEM-sensitive ATPase activities, as well as diffusive water flux rates. Unidirectional Na^+ influx and Na^+ efflux decreased during hypoxia in freshwater, but net Na^+ flux remained unchanged. Net loss rates of Cl^-, K^+ and ammonia were also attenuated in hypoxia, suggesting both transcellular and paracellular reductions in permeability. These reductions appeared to be regulated phenomena as fluxes were restored immediately in normoxia. Na^+ flux rates increased during hypoxia in 11 ppt, but decreased in 35 ppt, the latter suggesting a similar response to hypoxia to that in freshwater. In summary, freshwater and seawater killifish experience a reduction in gill permeability, as seen in other hypoxia-tolerant species. Fish acclimated to isosmotic salinity increased Na^+ influx and efflux rates, as well as paracellular permeability in hypoxia, responses in accord with the predictions of the classic osmorespiratory compromise.

KEY WORDS: Ion regulation, Respiratory gas exchange, Mummichog, Trade-offs

INTRODUCTION

The teleost fish gill is a multifunctional organ that is the primary site for ion and gas exchange in addition to playing a central role in acid–base balance and nitrogenous waste excretion (Evans, 2005). When needed, branchial oxygen exchange can be improved by increasing water flow across the gills (ventilation) and also changing the rate and pattern of gill blood flow (perfusion) (Perry et al., 2009). A reduction in heart rate and increase in cardiac stroke volume can lead to a recruitment of otherwise unperfused lamellae (Booth, 1978),

thereby increasing the functional surface area and reducing the blood-to-water diffusion distance for oxygen. However, an exacerbation of the unfavorable ion and water flux can occur. As stated in the classic first paper on this topic (Randall et al., 1972) 'Any change in the pattern of blood and water flow which reduces diffusion distance or increases the functional exchange area between blood and water will increase the rate of ion and water diffusion, unless there are compensatory reductions in the permeability of the gill epithelium'. This functional trade-off in optimal gill function has been termed the osmorespiratory compromise (Randall et al., 1972; Gonzalez and McDonald, 1992).

To date, the osmorespiratory compromise has been relatively well characterized in response to exercise. In the highly aerobic freshwater rainbow trout (*Oncorhynchus mykiss*), increases in swimming activity led to elevations in ion and water flux (Wood and Randall, 1973a,b,c; Gonzalez and McDonald, 1992; Postlethwaite and McDonald, 1995; Onukwufor and Wood, 2018).

However, fewer studies have looked at this phenomenon in response to the reduction of oxygen in the water. In hypoxia, fish improve the conditions for oxygen uptake by ventilating more water (Perry et al., 2009), and by changing blood flow patterns at the lamellae so as to increase functional surface area and decrease diffusion distance for exchange (Booth, 1978; Nilsson et al., 1995; Sundin and Nilsson, 1998). A likely consequence of these mechanisms is again a disturbance of ion and water balance as a result of the osmorespiratory compromise. Indeed, when exposed to hypoxia, rainbow trout experienced an increase in ion loss (Thomas et al., 1986; Iftikar et al., 2010; Robertson et al., 2015a), an effect that was paralleled by modifications in the gill epithelium, where ionocytes (mitochondria-rich cells) became more exposed, thereby increasing in surface area (Iftikar et al., 2010; Matey et al., 2011). In contrast, the Amazonian oscar (*Astronotus ocellatus*), a hypoxia-tolerant fish, exhibited a decrease in branchial ion and water flux in hypoxia (Wood et al., 2009; De Boeck et al., 2013; Robertson et al., 2015b). In addition, a reduction in the exposed surface area of ionocytes, due to pavement cell modifications, was observed at the gills (Wood et al., 2009; Matey et al., 2011; De Boeck et al., 2013). These responses occurred despite the fact that the oscar increased ventilation and the O_2 transfer factor of the gills (an index of effective gill O_2 permeability) during hypoxia (Scott et al., 2008a; Wood et al., 2009). These data suggest that hypoxia-tolerant fishes may circumvent or decouple the osmorespiratory compromise, by recruiting specific mechanisms at the level of the gill, preventing a disruption in the ionic balance, while gas exchange in hypoxia remains unaffected.

A few studies have examined the osmorespiratory compromise in seawater (SW) (Sardella and Brauner, 2007). Fish in SW are hypo-osmotic, contrary to what is seen in freshwater (FW). Therefore, it has always been thought that fish would face a net ion loading and water loss during hypoxia and exercise, given the reversed nature of the ionic gradients between fish and environment (Gonzalez, 2011). The few

[1]Department of Zoology, The University of British Columbia, Vancouver, BC, Canada V6T 1Z4. [2]Department of Anesthesiology and Perioperative Medicine, University of Rochester Medical Center, Rochester, NY 14642, USA. [3]Department of Biology, McMaster University, Hamilton, ON, Canada L8S 4K1.

*Author for correspondence (mussoigi@ualberta.ca)

M.G., 0000-0002-8163-3285; J.O.O., 0000-0003-4776-5003; P.M.S., 0000-0002-5237-8836; C.M.W., 0000-0002-9542-2219

Journal of Experimental Biology

1

experimental studies addressing the osmorespiratory compromise in SW have supported this conclusion (Farmer and Beamish, 1969; Stevens, 1972; Wood et al., 2019). Additionally, there has been no research on this phenomenon at the isosmotic salinity (the salinity at which the concentration gradient between the body fluids and external water is minimal). In theory, the osmorespiratory compromise at this salinity should be negligible, as no net movement of ions and water between the plasma and the environment should occur. A goal of the present study was to address these knowledge gaps.

Our overall goal was to increase our understanding of the ionoregulatory aspects of the osmorespiratory compromise during hypoxia across a range of salinities. We chose the Atlantic killifish, also known as the mummichog, *Fundulus heteroclitus*, as our model, because of its outstanding euryhalinity (Marshall, 2013) and its exceptional tolerance of hypoxia (Cochran and Burnett, 1996; Richards et al., 2008; McBryan et al., 2016). Killifish are native to estuaries and salt marshes but often enter rivers and creeks. In these environments, they can encounter variations in salinity and dissolved oxygen. In recent studies, we found that salinity affected killifish oxygen consumption and hypoxia tolerance (Giacomin et al., 2019) and also water exchange rates (Wood et al., 2019). Key findings from these two studies were that killifish increased gill ventilation during hypoxia, and exhibited the classic hypoxic bradycardia. Acclimation to FW led to reductions in hypoxia tolerance, likely due to a decrease in gill respiratory surface area and the presence of a greater interlamellar cell mass. Acclimation to 11 ppt (i.e. the isosmotic salinity for killifish) proved to be the most advantageous for respiratory gas exchange.

With this background in mind, our overall hypothesis was that there is a trade-off between efficient gas exchange and ion/water balance at the gills (osmorespiratory compromise) and the nature of this trade-off is flexible, depending on environmental salinity and oxygen levels. This hypothesis led to several predictions. Our first prediction was that killifish would reduce gill ion permeability in acute hypoxia, minimizing the flux of ions and water in both FW and SW, as seen in other hypoxia-tolerant species. Second, we predicted that in FW and SW, killifish would decrease the exposed surface area of ionocytes when exposed to hypoxia, so that respiratory surface area could be maintained while ion permeability was reduced, thereby avoiding the negative osmoregulatory effects of the osmorespiratory compromise. Lastly, we posited that in killifish acclimated to the isosmotic salinity, the effects of the osmorespiratory compromise would be minimal so that permeability could be increased without incurring negative osmoregulatory effects of the osmorespiratory compromise.

MATERIALS AND METHODS
Experimental animals
The experiments were performed throughout the year, from multiple field collections (April to October), between 2014 and 2018. All procedures were approved by the University of British Columbia Animal Care Committee (AUP A14-0251) and complied with the guidelines of the Canada Council for Animal Care. *Fundulus heteroclitus macrolepidotus* (Walbaum 1792) (northern subspecies) were collected by beach seine from a brackish estuary near Hampton, NH, USA, by Aquatic Research Organisms (Inc.) and air-shipped to the University of British Columbia, where they were held initially in 20 ppt water, as used by the supplier. They were later directly transferred to their experimental salinities, and held there for at least 6 weeks in each salinity prior to experimentation. There were no mortalities. Fish were held in 120 l glass tanks, containing FW (0 ppt: recirculating, charcoal-filtered dechlorinated Vancouver tap water containing mmol l^{-1}: [Na$^+$]=0.09, [Cl$^-$]=0.10,

[Ca^{2+}]=0.13, [Mg^{2+}]=0.01) or FW mixed with Instant Ocean Aquarium Salt (Instant Ocean, Spectrum Brands, Blacksburg, VA, USA) up to 11 ppt (mmol l^{-1}: [Na$^+$]=146, [Cl$^-$]=196, [Ca^{2+}]=4.3, [Mg^{2+}]=21.0) or SW (35 ppt; mmol l^{-1}: [Na$^+$]=459, [Cl$^-$]=663, [Ca^{2+}]=12.4, [Mg^{2+}]=53.6). Fish were fed daily with commercial flakes (Nutrafin Max Tropical Flakes) and fasted for at least 24 h prior to experiments. Salinity in the tanks and in the water prepared for experiments was monitored with a conductivity meter (Cond 3310, WTW, Xylem Analytics, Weilhem, Germany). The photoperiod was 12 h light:12 h dark, and the temperature during both acclimation and experimentation was 18–20°C. Water P_{O_2} was monitored during acclimation and throughout all experiments using a handheld oxygen meter (Accumet AP84, Fisher Scientific, Toronto, ON, Canada).

Influence of hypoxia and salinity on plasma ion composition and gill ionoregulatory enzymes
Fish (n=8 at each salinity and O$_2$ level) were held in individual plastic containers whose sides were replaced with a plastic mesh for free water flow. These were placed in 30 l darkened Plexiglas tanks overnight, one for each acclimation salinity (FW, 11 ppt and SW). The water in each 30 l tank was aerated and continuously recirculated by a small submersible water pump. Approximately 80% of the water was replaced prior to the start of the trial to avoid nitrogenous-waste build-up. P_{O_2} was either maintained at normoxia (~155 Torr=20.7 kPa) or reduced from normoxia to hypoxia (15±2 Torr=2 kPa) over a 30 min period and maintained at a constant level with bubbling of N$_2$ or air. Fish were kept in hypoxia for 3 h, and at the end of the experiment were immediately killed with an overdose of neutralized MS-222 (Syndel Laboratories, Nanaimo, BC, Canada). Normoxic fish underwent the same protocol, but P_{O_2} was kept at normoxia. Blood samples (~100 µl) were quickly drawn by caudal puncture using a modified gas-tight Hamilton 100 µl syringe (Reno, NV, USA). Two 5 µl micro-hematocrit tubes were filled with blood and centrifuged at 10,000 *g* for 10 min. The remainder of the blood was also centrifuged (5 min, 10,000 *g*), and the separated plasma was then flash-frozen in liquid N$_2$. Additionally, the left-hand side of the gill basket was excised and also flash-frozen in liquid N$_2$. Plasma and tissue samples were kept at −80°C until analysis of plasma ion concentrations and osmolality, plasma lactate concentration, and gill Na$^+$/K$^+$-ATPase and H$^+$-ATPase activity (described below). The right-hand side of the gill basket was immediately fixed in Karnovsky's fixative for 24 h at 4°C. The samples were transferred to 0.1 mol l^{-1} sodium cacodylate and stored at 4°C until use. For scanning electron microscopy (SEM), sections of the center part of the second gill arch were progressively dehydrated in ethanol, critically point dried with CO$_2$, and then sputter-coated with 9 nm of gold–palladium. Samples were imaged on a Hitachi S-4700 Field Emission Scanning Electron Microscope (Tokyo, Japan) at 2000× magnification.

Influence of hypoxia and salinity on diffusive water flux rates
Separate groups of fish (n=12 at each salinity and O$_2$ level) were used to measure diffusive water flux rates in animals acclimated to FW, 11 ppt and SW, in normoxia and exposed to hypoxia. Groups of n=6 fish were placed in darkened 1 l containers, at the acclimation salinity and dosed with 20 µCi l^{-1} of ^{3}H$_2$O (Amersham Pharmacia Biotech, Little Chalfont, UK). This loading period was performed overnight, while the chambers were constantly aerated, and temperature controlled to 20°C. Preliminary trials demonstrated that ^{3}H$_2$O concentration in the fish's body water pool and in the external water of the loading bath had reached an equilibrium within 6 h. After the loading period, the fish were quickly rinsed in non-

radioactive water, and then transferred to individual darkened 250 ml containers, each filled with water at the appropriate salinity and P_{O_2}, which served as the experimental chambers. Water P_{O_2} was set to normoxia (155 Torr) or hypoxia (15±2 Torr) and was kept at these levels for the following 60 min. Water samples (5 ml) were taken every 5 min for 60 min. Normoxia was restored and a final water sample was taken at 8 h, by which time the radioactivity in the fish had completely equilibrated with the external water. Scintillation fluor (Optiphase, Perkin Elmer, Waltham, MA, USA) was added to the water samples in a 2:1 (fluor:water) ratio, and samples were stored in the dark for a minimum of 2 h to eliminate chemiluminescence prior to scintillation counting for beta emissions (Beckman Coulter, LS6500, Wellesley, MA, USA). Tests showed that quench was constant.

Diffusive water flux rates were calculated following methods described in Giacomin et al. (2017) and Onukwufor and Wood (2018). The rate of disappearance of ^3H_2O from the fish was calculated from the ^3H_2O washout from the animal as measured by its appearance in the water. The rate constant of ^3H_2O turnover (k: fraction of body water h^{-1}) was calculated as:

$$k = (\ln R_1 - \ln R_2)/(t_1 - t_2), \quad (1)$$

where R_1 and R_2 are total ^3H_2O radioactivity (counts min^{-1}, cpm) in the fish (see below) at times t_1 and t_2 (h). Data were used only over the range where efflux was linear (up to 40 min from the start of experiment). The total volume of the system was estimated as the measured volume of external water (experimental container) plus the volume of the fish (assuming 1 g=1 ml). The water sample that was taken at 8 h (after complete washout and equilibration had occurred) plus all radioactivity removed by sampling during the experiment were used to calculate the total amount of ^3H_2O radioactivity that had been loaded into the fish (R_{total}). Therefore, the radioactivity remaining in the fish at each time interval (R_1, R_2, R_x) was then calculated by subtracting the ^3H_2O measured in the water from R_{total} at each time interval. The product of $k \times 100$ is reported as the percentage of the body water pool turned over per hour. This turnover can be converted to ml g^{-1} h^{-1} by multiplying by 0.80 ml g^{-1}, based on the estimates of Holmes and Donaldson (1969), Isaia (1984) and Olson (1992) that water comprises about 80% of body mass.

Influence of hypoxia and salinity on gill paracellular permeability and drinking rate

Separate groups of fish (n=8 at each salinity and O_2 level) were used to measure gill paracellular permeability and drinking rate, using radiolabeled polyethylene glycol ([^3H]PEG-4000) following methods developed by Robertson and Wood (2014). Briefly, the appearance of radioactivity in the carcass was used as a measurement of gill paracellular permeability, while the appearance of radioactivity in the gut was used to measure drinking rate. Groups of fish (n=8) were exposed for 3 h in 1 l of water at the acclimation salinity labeled with 25 μCi l^{-1} [^3H]PEG-4000 (Amersham). Preliminary experiments demonstrated that there was no rectal excretion of [^3H]PEG-4000 in that time. Fish were allowed to settle in the aerated light-shielded experimental container for 2 h in normoxia prior to the addition of radioactivity. After that, P_{O_2} was either maintained at 155 Torr by air bubbling or quickly reduced to 15±2 Torr by N_2 bubbling, and when P_{O_2} reached hypoxic levels, the radioisotope was added. Water samples (5 ml) were taken at 0, 1.5 and 3 h for scintillation counting. At the end of 3 h, all fish were killed by an overdose of neutralized MS-222, rinsed in radioisotope-free water, blotted dry and kept on ice until

dissection. The gastrointestinal tract was tied at both ends (to avoid content loss) and excised. The gut and remaining carcass were weighed separately, and digested in sealed vials with 2 mol l^{-1} HNO_3 for 48 h at 60°C, with periodic agitation. The digests were then centrifuged (5000 g for 5 min) and the clear supernatant was aliquoted for scintillation counting. Water and carcass digest samples (2 ml), and gut digest samples (0.2 ml) were dosed with 10 ml of scintillation cocktail (Ultima Gold AB, Perkin Elmer) and read on a scintillation counter (LS6500, Beckman Coulter). Radioactivity of the tissue digests was quench-corrected to the same counting efficiency as water samples based on a quench curve constructed previously with different amounts of tissue digest.

[^3H]PEG-4000 gill clearance rate (CR, μl g^{-1} h^{-1}) as a proxy for branchial paracellular permeability was calculated as follows:

$$[^3H]PEG\text{-}4000\ CR\ = (cpm\ in\ carcass)/(mean\ water\ cpm/\mu l \times M \times T), \quad (2)$$

where cpm in carcass is the total amount of radioactivity in the carcass, M is the fish body mass (g) and T is time (h).

[^3H]PEG-4000 drinking rate (DR, μl g^{-1} h^{-1}) was calculated in a similar manner as follows:

$$[^3H]PEG\text{-}4000\ DR = (cpm\ in\ gut)/(mean\ water\ cpm/\mu l \times M \times T), \quad (3)$$

where cpm in gut is the total amount of radioactivity in the gut.

Unidirectional and net ion flux rates in killifish acclimated to FW, 11 ppt and SW

Previous studies (Wood and Laurent, 2003; Wood, 2011) have demonstrated that it is necessary to use different methods to measure unidirectional flux of Na^+ in saline waters versus FW, and we adopted those methods in the present study. All techniques described below were employed to meet the experimental criteria outlined in Wood (2011). Briefly, the specific activity (ratio of radioisotopic Na^+ to 'cold' Na^+) in the compartment where radioactivity appearance was being monitored, either water or fish, needs to remain less than 10% of the specific activity in the compartment to which radioactivity was added, so as to prevent radio-isotopic back flux. The difficulty of meeting this criterion when measuring ^{22}Na flux in 11 ppt and full-strength SW constrained our ability to replicate all the experiments performed in FW at those salinities. A limitation of these approaches is that because the methods differ for influx and efflux determinations, and must be performed on different fish over different time frames (0.5 h for influx, 3 h for efflux), influx and efflux rate measurements may not be quantitatively comparable to one another. Therefore comparisons should only be made of influx rates across treatments, and efflux rates across treatments, and not of efflux rates versus influx rates within treatments. Therefore, our investigation of the unidirectional ion flux responses to hypoxia is more detailed in FW than in 11 ppt or SW. Furthermore, our previous study (Giacomin et al., 2019) indicated that the impacts of the hypoxia-induced osmorespiratory compromise are most intense in FW killifish. All ^{22}Na measurements were made with a gamma counter (1470 Wallac-Wizard, Perkin Elmer, Waltham, MA, USA).

Separate groups of fish (n=15 at each salinity and O_2 level) were used for each of the experimental series described below. For all experimental flux measurements, fish were held in individual 250 ml plastic containers, served with aeration tubing, darkened with black plastic and partially submerged in a wet table to ensure temperature control. The water surface was covered in plastic so as

to avoid oxygen diffusion from the air, and to prevent the fish from performing aquatic surface respiration.

Ion flux in FW-acclimated killifish

In FW, Na^+ influx ($J_{influx}^{Na^+}$) was measured by monitoring the disappearance of radioactivity from the water. To that end, fish were transferred to the containers described above and allowed to acclimate overnight under flow-through conditions. Prior to the start of the experiment, flow-through ceased, the water level was set at 250 ml, and 5 μCi ^{22}Na was added. Water samples (5 ml) were collected hourly for 3 h and stored for measurement of radioactivity, total Na^+, Cl^-, K^+ and ammonia concentrations.

At 3 h, the water was replaced with water that had been pre-equilibrated with N_2 to 15±2 Torr (hypoxia) and dosed with the same amount of ^{22}Na. Water samples (5 ml) were collected again hourly for another 3 h. At the end of the hypoxia exposure time, the containers were quickly bubbled with air and normoxia was restored within 5 min. Recovery trials lasted for another 3 h. A control group (normoxia) was established, in which all the experimental procedures were conducted similarly, with the exception that the animals were maintained in normoxia throughout the whole 9 h duration of the trial. Fish were weighed at the end of the experiment. At each 1 h period, the unidirectional Na^+ influx rate (nmol g^{-1} h^{-1}) was calculated as:

$$J_{influx}^{Na^+} = [(cpm_i - cpm_f) \times V]/(mean\ SA_{ext} \times T \times M), \quad (4)$$

where cpm_i and cpm_f are the ^{22}Na count per ml in the water at the start and end of each 1 h period, respectively, V is the volume in each period (l), mean SA_{ext} is the mean external specific activity of Na^+ (cpm nmol^{-1}), T is time (h) and M is the body mass (g).

Na^+ net flux rates (nmol g^{-1} h^{-1}) were determined from the concentration of total 'cold' Na^+ in the water (nmol l^{-1}) and calculated using the following equation:

$$J_{netflux}^{Na^+} = [([Na^+]_i - [Na^+]_f) \times V]/(T \times M), \quad (5)$$

where $[Na^+]_i$ and $[Na^+]_f$ are the Na^+ concentration of the water (nmol l^{-1}) at the start and end of each 1 h period, respectively, V is the volume in each period (l), T is time (h) and M is the body mass (g).

Unidirectional Na^+ efflux rates (nmol g^{-1} h^{-1}) were calculated as follows:

$$J_{efflux}^{Na^+} = J_{netflux}^{Na^+} - J_{influx}^{Na^+}, \quad (6)$$

where $J_{net\ flux}^{Na^+}$ was calculated by Eqn 5 and $J_{influx}^{Na^+}$ by Eqn 4.

Cl^-, K^+ and total ammonia ($NH_3 + NH_4^+$) net flux rates (nmol g^{-1} h^{-1}) were determined from the concentrations in the water (nmol l^{-1}) and calculated using an equation analogous to Eqn 5.

Unidirectional Na^+ influx and efflux in 11 ppt- and SW-acclimated killifish

Separate groups of fish (n=15 at each O_2 and salinity level) were used to determine the influence of hypoxia on the unidirectional influx of Na^+ in killifish acclimated to SW (35 ppt) or 11 ppt. $J_{influx}^{Na^+}$ was determined by monitoring the appearance of radioactivity in the fish. Note that Wood (2011) concluded that approximately 80–90% of Na^+ influx occurs across the gills, and 10–20% across the gut in seawater killifish; the dominance of the gills would be even greater at intermediate salinity where drinking rate is lower. In order to avoid radiotracer recycling and maintain the 10% specific activity criterion (see above), a flux period of 0.5 h was employed (Wood

and Laurent, 2003; Wood, 2011). Fish were allowed to settle in the containers described above overnight under flow-through conditions, and water volume was set to 250 ml prior to the start of the experiment with normoxic (155 Torr) or hypoxic (15±2 Torr) water. Fish were exposed to these conditions for 2.5 h in order to mimic the duration of the hypoxia exposure employed in fish acclimated to FW. At 2.5 h, 10 μCi ^{22}Na was added to the water. Water samples were taken at the start and end of the 0.5 h flux period and stored for measurement of radioactivity and total Na^+ concentration. The fish were then rinsed in non-radioactive water of the appropriate salinity (11 ppt or SW) for 1 min, killed in neutralized MS-222 (0.5 g l^{-1}), blotted dry, weighed and processed for measurement of whole-body radioactivity (^{22}Na). Unidirectional influx rates (nmol g^{-1} h^{-1}) were calculated as follows:

$$J_{influx}^{Na^+} = \Sigma(cpm\ in\ fish)/(mean\ SA_{ext} \times T \times M), \quad (7)$$

where $\Sigma(cpm\ in\ fish)$ is the total ^{22}Na radioactivity in the fish, mean SA_{ext} is the mean external specific activity of Na^+ (cpm nmol^{-1}), T is time (h) and M is body mass (g).

Separate groups of fish (n=15 at each O_2 and salinity level), different from those used for influx, were used to determine the influence of hypoxia on the unidirectional efflux of Na^+ in killifish acclimated to SW (35 ppt) or 11 ppt. $J_{efflux}^{Na^+}$ was determined by loading the fish with ^{22}Na, and then monitoring the appearance of radioactivity in the water. To load ^{22}Na into the fish, they were incubated overnight in batches of 8 in 80 μCi ^{22}Na l^{-1} at the salinity of acclimation, in a 1.5 l Erlenmeyer glass container. The loading chamber was aerated and shielded from light. Previous tests showed that a minimum of 10 h was needed for complete equilibration between the fish and the external media. After incubation, fish were quickly rinsed in non-radioactive water, then transferred to the same experimental chambers as described above, each containing 250 ml of SW at the appropriate salinity. Water samples were taken every 0.5 h for 1.5 h, and then either normoxic (155 Torr) or hypoxic (15±2 Torr) water was used to replace the water in the chambers. The volume was again adjusted to 250 ml, and additional water samples were taken every 0.5 h for 3 h. This was done so as to provide the fish with the same time frame of hypoxia exposure as described for fish acclimated to 0 ppt. At the end of the experiment, fish were rinsed in non-radioactive water for 1 min, killed in neutralized MS-222 (0.5 g l^{-1}), blotted dry, weighed and processed for measurement of whole-body radioactivity (^{22}Na). Unidirectional efflux rates were calculated as follows (Wood and Laurent, 2003):

$$J_{efflux}^{Na^+} = [(k \times \Sigma Z \times F)/M], \quad (8)$$

where k is the rate constant of radioactivity lost (% exchangeable whole-body Na^+ pool h^{-1}) by the fish per unit time, ΣZ is the total internal Na^+ pool (nmol g^{-1}), F is the fractional labeling of that pool by the radioisotope and M is the body mass (g). ΣZ and F were obtained from Wood and Laurent (2003). The total radioactivity appearance in the water, including that removed in water sampling, when added to the radioactivity measured in the fish carcass, yielded the total radioactivity in the fish at the start of the experiment. The slope of the natural logarithm of the loss of this radioactivity versus time provides the rate constant (k) of radioactivity lost, and it was calculated using an equation analogous to Eqn 1. Only data obtained during the hypoxia period were used.

Ammonia net flux rate ($J_{net\ flux}^{amm}$: nmol g^{-1} h^{-1}) was determined from the measured total concentrations of ammonia (NH_3 and NH_4^+) in the water and calculated as described for the FW trials above. Net flux rates of Na^+, K^+ and Cl^- were not measured in 11 ppt and SW

because of the background ionic concentrations being too high to reliably detect fish-induced changes.

Analytical techniques

Water Na^+ and K^+ concentrations (nmol l^{-1}), and plasma Na^+ concentrations (mmol l^{-1}) were determined by atomic absorption (1275 Atomic Absorption Spectrophotometer, Varian, Mulgrave, VIC, Australia) using certified commercial standards (Fluka Analytical, Sigma-Aldrich, St Louis, MO, USA). Plasma osmolality (mOsm kg^{-1}) was measured using a Wescor vapor pressure osmometer and standards (Wescor 5100C, Logan, UT, USA). Water (μmol l^{-1}) and plasma (mmol l^{-1}) Cl^- were determined colorimetrically using the mercury–thiocyanate method described by Zall et al. (1956). Ammonia concentration (μmol l^{-1}) in the water was measured using the colorimetric method of Verdouw et al. (1978).

Plasma lactate concentration (mmol l^{-1}) was determined as described by Bergmeyer (1983). Briefly, plasma samples were deproteinized with 8% perchloric acid, centrifuged briefly to precipitate proteins (8 min, 5000 g), and assayed in triplicate on a microplate spectrophotometer (SpectraMAX Plus; Molecular Devices, Menlo Park, CA, USA) with a reaction buffer solution (0.18 mol l^{-1} glycine, 0.15 mol l^{-1} hydrazine, 0.015 βNAD^+, 15 U ml^{-1} lactate dehydrogenase, pH 9.4). The reaction mixture was incubated for 60 min at 37°C, and lactate concentration was determined against a standard curve.

Na^+/K^+-ATPase and NEM-sensitive ATPase activity (μmol ADP mg^{-1} protein h^{-1}) were measured in gill tissues according to protocols described in McCormick (1993) and Lin and Randall (1993), respectively. Tissues were homogenized (1:10 w/v) in ice-cold buffer solution [50 mmol l^{-1} imidazole, 125 mmol l^{-1} sucrose and 5 mmol l^{-1} EGTA (pH 7.3)], centrifuged (5000 g, 3 min, 4°C), and supernatants kept on ice throughout the analysis. All samples were assayed within 2 h of thawing and homogenization. Ouabain (0.05 mmol l^{-1}) was used as an inhibitor of Na^+/K^+-ATPase with sodium azide (NaN_3, 5.15 mmol l^{-1}) as an inhibitor of ATP synthase. N-Ethylmaleimide (NEM) at 1.03 mmol l^{-1} was used as an inhibitor of H^+-ATPase. An important caveat to note is that at this high concentration, NEM may not be a specific inhibitor of only V-type H^+-ATPase and might inhibit other ATPases (Forgac, 1989; Lin and Randall, 1993). For this reason, in accord with Tipsmark et al. (2004), we describe these results as NEM-sensitive ATPase throughout; all the tissue samples were analyzed using the same method, so the comparisons between treatments remain valid. Activity was calculated by the difference between the amounts of adenosine diphosphate (ADP) produced in control and inhibited reactions. Absorbance was monitored at 10 s intervals over 5 min (25°C) on the same microplate spectrophotometer. Protein concentration in homogenates was determined using the Bradford reagent (Sigma-Aldrich).

For the measurement of hematocrit (Hct), micro-hematocrit tubes (2×5 μl) were centrifuged (10,000 g, 10 min) and Hct was measured as the percentage of packed red blood cells (%RBC) within the total blood volume.

Morphometric quantification of exposed ionocyte surface area and density (number of ionocytes per mm^2) was performed on randomly selected areas of the afferent surface of filaments near the respiratory lamellae. The individual exposed surface area of approximately 50 ionocytes was measured over randomly selected areas of the epithelium for each fish at 2000× magnification. The surface area of individual pavement cells (PVCs) was also measured on randomly selected cells from each of five fish on the same micrographs. Microridge density on the surface of PVCs was calculated on 20

random cells from each of five fish as the total number of intercepts (for the whole cell) of microridge profiles on a lattice grid composed of 2.82×2.82 μm squares superimposed on the micrograph. This result (total number of intercepts per individual cell) was then divided by the individual PVC surface area (μm^2), yielding intercepts per μm^2 of PVC surface area. The exposed ionocyte fractional surface area was calculated by multiplying ionocyte surface area (μm^2 per cell) by ionocyte density (cells μm^{-2}). All measurements were performed using ImageJ v152 (Public domain).

Statistical analyses

All data are shown as means±s.e.m. (n=number of animals). Assumptions of parametric statistics (data normality and homogeneity of variances) were checked, and if not met, data were transformed using a log transformation. Data were analyzed using one-way ANOVA, two-way ANOVA or repeated measures ANOVA as appropriate. Detailed results of the statistical tests and *post hoc* analysis are shown in figure captions. When applied, one-way ANOVA was followed by a Tukey *post hoc* test. Two-way ANOVA was followed by a Bonferroni *post hoc* test. Mean values were considered significantly different when $P<0.05$.

RESULTS

Plasma ions and enzyme activity

Salinity acclimation exerted a significant overall effect on plasma ions and osmolality (Fig. 1). Under normoxia, plasma [Na^+] was significantly higher in SW-acclimated fish (~150 mmol l^{-1}) than in FW-acclimated fish (~135 mmol l^{-1}) (Fig. 1A). Plasma Cl^- followed a similar trend, where 11 ppt-acclimated fish showed an intermediate value between those of FW- and SW-acclimated fish (~110 and ~140 mmol l^{-1}, respectively; Fig. 1B). Neither plasma [Na^+] (Fig. 1A) nor plasma [Cl^-] (Fig. 1B) was significantly affected by hypoxia at any salinity. There was no significant interaction between salinity and oxygen for plasma [Na^+] and [Cl^-] (Fig. 1A,B). Plasma osmolality was similar in fish acclimated to 11 ppt and SW (35 ppt) (~375 mOsm kg^{-1}) and both were significantly higher than in FW-acclimated fish (~340 mOsm kg^{-1}; Fig. 1C). There was no significant effect of hypoxia and no significant interaction between oxygen and salinity on plasma osmolality (Fig. 1C).

Hypoxia exposure had a significant overall effect on both gill Na^+/K^+-ATPase and NEM-sensitive ATPase activity, with lower activity in hypoxia than normoxia (Fig. 2). Two-way ANOVA did not detect a significant effect of salinity acclimation on either Na^+/K^+-ATPase or NEM-sensitive ATPase activity, and there was no significant interaction between salinity and oxygen.

Blood Hct and plasma lactate

Hypoxia exposure had a significant overall effect on blood Hct, while salinity acclimation did not (Fig. 3A). At all salinities, hypoxia exposure caused an increase in blood Hct, which was significantly different from normoxic values in 11 ppt and SW (35 ppt) (Fig. 3A).

There were significant overall effects of both salinity and hypoxia on plasma lactate concentration (Fig. 3B); however, plasma lactate was significantly elevated only in FW- and 11 ppt-acclimated fish. Fish in 11 ppt showed the largest difference in plasma lactate between normoxia and hypoxia exposure (60% increase), followed by fish acclimated to FW (46% increase; Fig. 3B).

Diffusive water flux rates, gill paracellular permeability and drinking rate

Salinity acclimation had a significant overall effect on the diffusive water flux rate (Fig. 4A). Water flux rate was the highest (~94% of
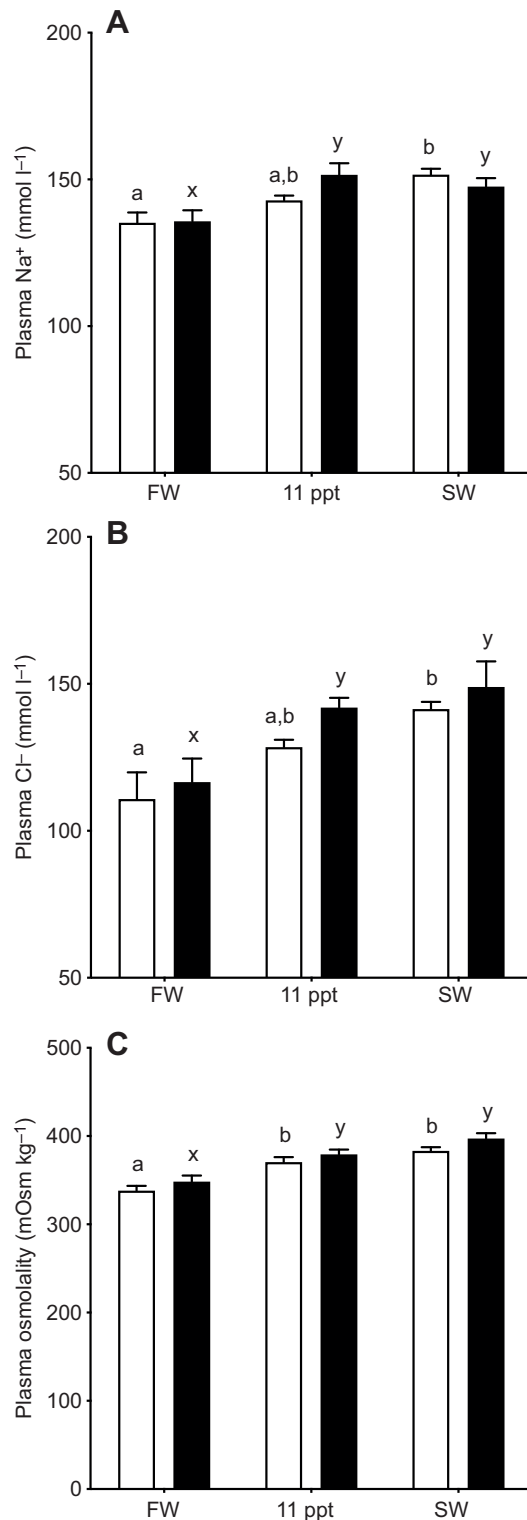
Fig. 1. Effect of salinity acclimation and hypoxia on plasma ions and osmolality. (A) Plasma sodium, (B) plasma chloride and (C) plasma osmolality in *Fundulus heteroclitus* acclimated to freshwater (FW, 0 ppt), 11 ppt and seawater (SW, 35 ppt) in normoxia (white bars) and exposed to hypoxia (black bars). Bars sharing the same lowercase letters are not statistically different at the same oxygen level. (Two-way ANOVA P-values – plasma Na^+: $P_{interaction}=0.1221$, $P_{oxygen}=0.5051$, $P_{salinity}<0.0001$; plasma Cl^-: $P_{interaction}=0.8137$, $P_{oxygen}=0.0909$, $P_{salinity}<0.0001$; plasma osmolality: $P_{interaction}=0.8878$, $P_{oxygen}=0.0217$, $P_{salinity}<0.0001$). Data are means±s.e.m. (n=8).
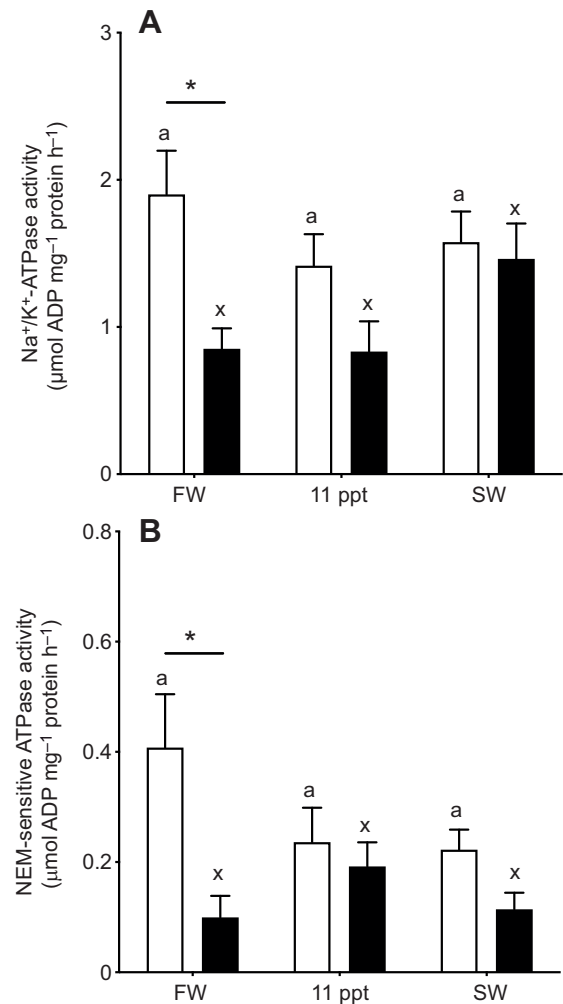
Fig. 2. Effect of salinity acclimation and hypoxia on enzyme activity. (A) Na^+/K^+-ATPase and (B) NEM-sensitive ATPase activity in *F. heteroclitus* acclimated to FW (0 ppt), 11 ppt and SW (35 ppt) in normoxia (white bars) and exposed to hypoxia (black bars). Bars sharing the same lowercase letters are not statistically different at the same oxygen level. (Two-way ANOVA P-values – Na^+/K^+-ATPase: $P_{interaction}=0.1356$, $P_{oxygen}=0.0037$, $P_{salinity}=0.2233$; NEM-sensitive ATPase: $P_{interaction}=0.0608$, $P_{oxygen}=0.0011$, $P_{salinity}=0.2622$). Asterisks indicate significant differences between normoxia and hypoxia at the same salinity (Bonferroni *post hoc* test). Data are means±s.e.m. (n=8).

the body water pool h^{-1}) in fish acclimated to FW, and significantly different from that of fish acclimated to 11 ppt and SW, which had similar rates ($\sim$57–47% h^{-1}; Fig. 4A). There was a significant decrease (30%) with hypoxia exposure in FW-acclimated fish, but no effect of hypoxia in fish acclimated to 11 ppt and SW (Fig. 4A).

There was an overall effect of salinity on gill clearance rates of [^{3}H]PEG-4000, an index of gill paracellular permeability, while under normoxia, FW- and SW-acclimated fish exhibited very similar rates and 11 ppt-acclimated fish had a significantly lower rate ($\sim$1.0 µl g^{-1} h^{-1}) (Fig. 4B). While hypoxia exposure did not have an overall effect on the [^{3}H]PEG-4000 gill clearance rate (Fig. 4B), at 11 ppt gill clearance rate was elevated (Fig. 4B).

Both salinity acclimation and hypoxia exposure had significant overall effects on drinking rate (Fig. 4C). Under normoxia, drinking rate was the lowest in FW ($\sim$0.15 µl g^{-1} h^{-1}), and approximately 40-fold higher ($\sim$6.1 µl g^{-1} h^{-1}) in SW (Fig. 4C). Drinking rate was decreased significantly with hypoxia exposure (88%) in SW (Fig. 4C).
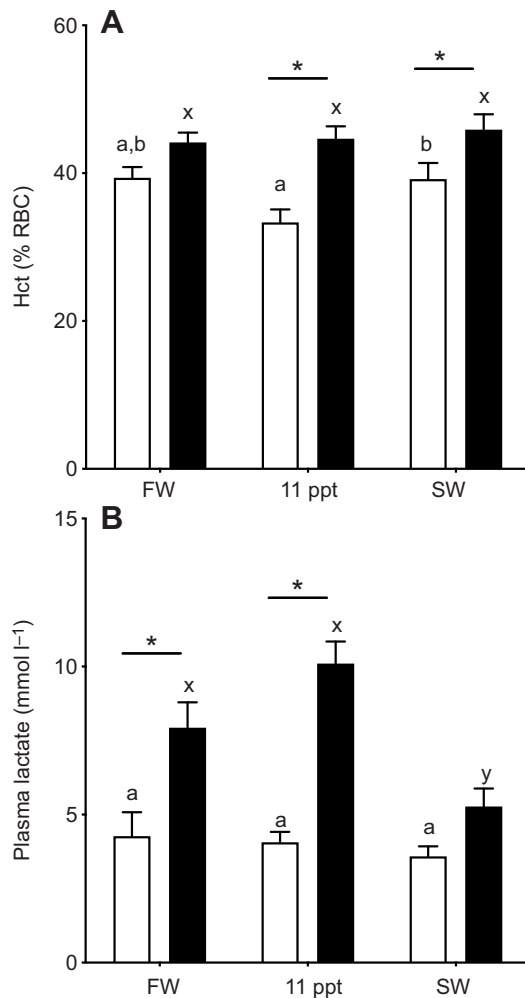
Fig. 3. Effect of salinity acclimation and hypoxia on blood hematocrit (Hct) and plasma lactate. (A) Hct (RBC, red blood cell) and (B) plasma lactate in *F. heteroclitus* acclimated to FW (0 ppt), 11 ppt and SW (35 ppt) in normoxia (white bars) and exposed to hypoxia (black bars). Bars sharing the same lowercase letters are not statistically different at the same oxygen level. (Two-way ANOVA *P*-values – hematocrit: $P_{interaction}=0.1845$, $P_{oxygen}<0.0001$, $P_{salinity}=0.1239$; lactate: $P_{interaction}=0.0051$, $P_{oxygen}<0.0001$, $P_{salinity}=0.0006$). Asterisks indicate significant differences between normoxia and hypoxia at the same salinity (Bonferroni *post hoc* test). Data are means±s.e.m. (*n*=8).

Unidirectional flux rates of Na⁺, and net flux rates of Cl⁻, K⁺ and ammonia

In FW, there were no significant changes in unidirectional flux rates of Na⁺ or the net flux rates of Cl⁻, K⁺ and ammonia in the fish subjected to the normoxic control sham procedures (data not shown). FW-acclimated killifish exhibited an average $J_{influx}^{Na^+}$ of 310 nmol g⁻¹ h⁻¹ in normoxia (Fig. 5A). In the first hour of hypoxia, $J_{influx}^{Na^+}$ did not change, but it decreased significantly by about 55% for the remainder of the hypoxia exposure (Fig. 5A). $J_{influx}^{Na^+}$ returned to pre-exposure levels as soon as fish were returned to normoxia (Fig. 5A). $J_{efflux}^{Na^+}$ showed a similar response pattern to that for influx, with an overall reduction in the second and third hours of hypoxia, and recovery to close to control levels upon re-instatement of normoxia (Fig. 5B). In normoxia, the average $J_{efflux}^{Na^+}$ was about −300 nmol g⁻¹ h⁻¹, and during hypoxia, it decreased significantly by 50% at the second hour, and by 36% at the third hour (Fig. 5B). The resulting net flux rates (~−25 nmol g⁻¹ h⁻¹) were therefore essentially unchanged with no significant differences among normoxia, hypoxia and recovery (Fig. 5C).
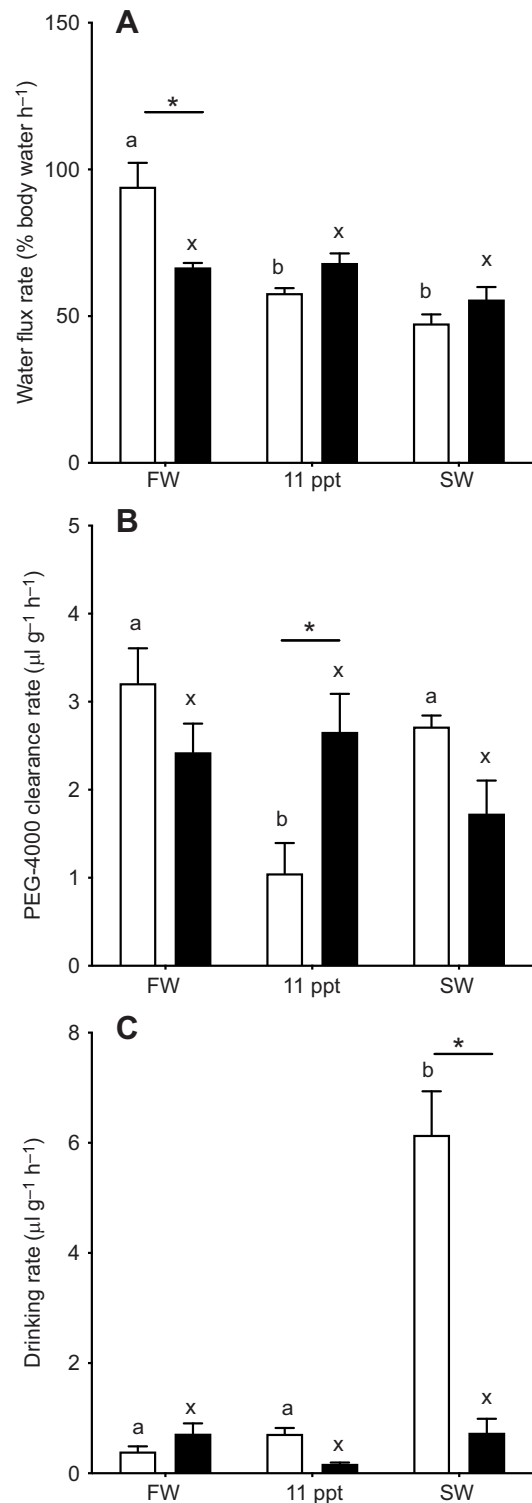

Fig. 4. Effect of salinity acclimation and hypoxia on water flux, gill paracellular permeability and drinking rate. (A) Diffusive water flux rate, (B) PEG-4000 clearance rate and (C) drinking rate in *F. heteroclitus* acclimated to FW (0 ppt), 11 ppt and SW (35 ppt) in normoxia (white bars) and exposed to hypoxia (black bars). Bars sharing the same lowercase letters are not statistically different at the same oxygen level. (Two-way ANOVA *P*-values – water flux rate: $P_{interaction}<0.0001$, $P_{oxygen}=0.3608$, $P_{salinity}<0.0001$; clearance rate: $P_{interaction}=0.0046$, $P_{oxygen}=0.8712$, $P_{salinity}=0.03733$; drinking rate: $P_{interaction}<0.0001$, $P_{oxygen}<0.0001$, $P_{salinity}<0.0001$). Asterisks indicate significant differences between normoxia and hypoxia at the same salinity (Bonferroni *post hoc* test). Data are means±s.e.m. (*n*=12 for A and *n*=8 for B,C).

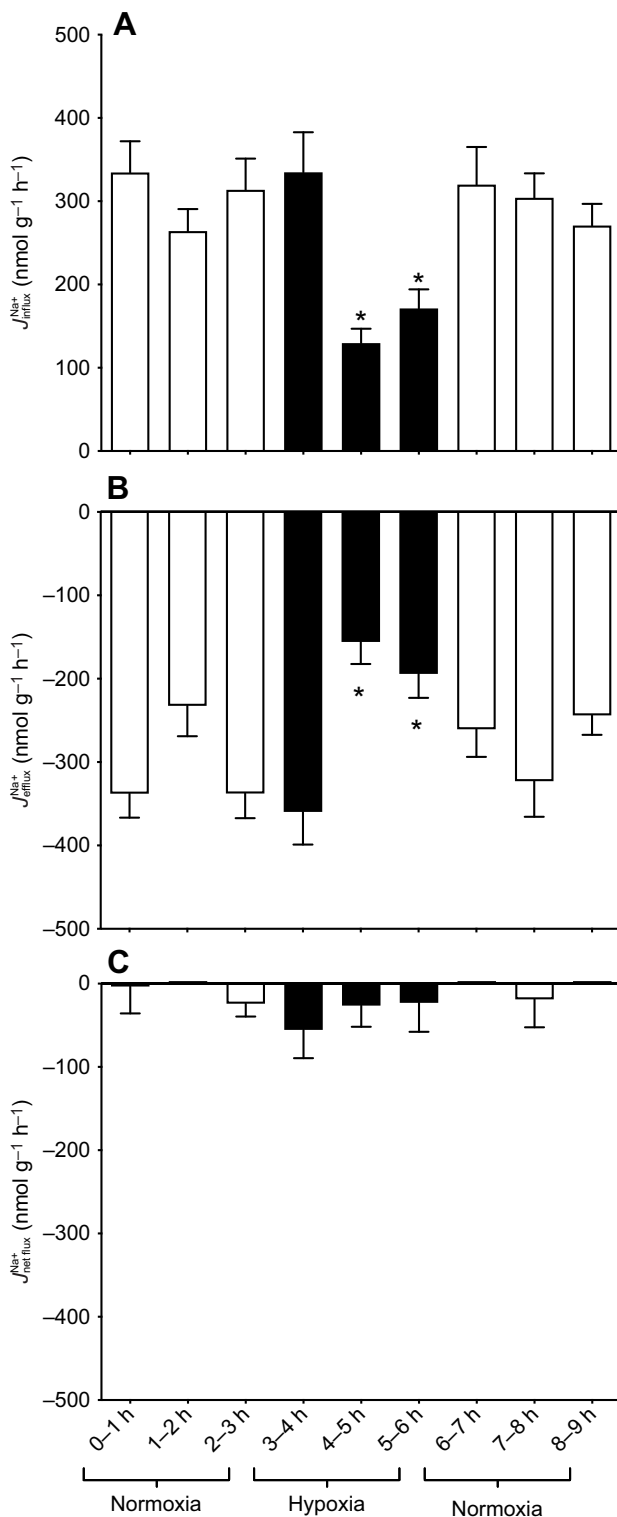**Fig. 5. Effect of hypoxia on unidirectional Na⁺ flux.** (A) Unidirectional sodium influx rate ($J_{influx}^{Na^+}$), (B) unidirectional sodium efflux rate ($J_{efflux}^{Na^+}$) and (C) sodium net flux rate ($J_{net\ flux}^{Na^+}$) in *F. heteroclitus* acclimated to FW (0 ppt). Fish were subjected to 3 h each of normoxia, hypoxia and normoxia. Asterisks indicate significant differences from the averaged starting normoxia period (Dunnett's test). Data are means±s.e.m. (*n*=15).

In normoxia, the average net Cl⁻ flux rate was −39 nmol g⁻¹ h⁻¹, and did not change in the first hour of hypoxia, but was significantly reversed to about +100 nmol g⁻¹ h⁻¹ in the second and third

hours (Fig. 6A). Cl⁻ net flux rate returned to pre-exposure levels once normoxia was restored. In normoxia, the net K⁺ flux rate was about −20 nmol g⁻¹ h⁻¹, and during hypoxia, it followed the same pattern as seen for unidirectional Na⁺ flux, and net Cl⁻ flux, where the rates were unchanged in the first hour, but decreased substantially (by about 70%) in the second and third hours (Fig. 6B). In recovery, the K⁺ flux rate was restored to levels similar to original in normoxia (Fig. 6B). The ammonia excretion rate was about −350 nmol g⁻¹ h⁻¹ in normoxia, and it significantly decreased by about 60% immediately upon hypoxia exposure (Fig. 6C). Ammonia excretion did not change during subsequent hypoxia, but increased immediately back to control levels once normoxia was restored (Fig. 6C).

In SW, only single values were obtained for unidirectional Na⁺ flux rates during normoxia and hypoxia, and net flux rates of Na⁺, K⁺ and Cl⁻ were not measured. In Fig. 7, we have shown the overall time-averaged unidirectional Na⁺ flux rates for normoxia and hypoxia of FW-acclimated killifish (from Fig. 5A,B) in order to make comparisons with fish acclimated to 11 ppt and SW. Note that the scale is broken to accommodate the wide range of values.

On average, $J_{influx}^{Na^+}$ in FW-acclimated fish was +310 nmol g⁻¹ h⁻¹, while in hypoxia this decreased to +210 nmol g⁻¹ h⁻¹ (Fig. 7A). The average $J_{efflux}^{Na^+}$ was −300 nmol g⁻¹ h⁻¹, while in hypoxia it decreased to −250 nmol g⁻¹ h⁻¹ (Fig. 7B). Fish acclimated to 11 ppt in normoxia showed a severalfold higher $J_{influx}^{Na^+}$ of +6400 nmol g⁻¹ h⁻¹, while in hypoxia this increased by 150% to +16,000 nmol g⁻¹ h⁻¹ (Fig. 7A). There was also a 92% increase in $J_{efflux}^{Na^+}$ in 11 ppt fish exposed to hypoxia (−5400 nmol g⁻¹ h⁻¹) in comparison to normoxia (−2800 nmol g⁻¹ h⁻¹; Fig. 7B). The $J_{influx}^{Na^+}$ in normoxia of SW-acclimated fish was about +22,000 nmol g⁻¹ h⁻¹, which decreased significantly by 13% when fish were exposed to hypoxia (Fig. 7A). In normoxia, $J_{efflux}^{Na^+}$ was approximately −12,000 nmol g⁻¹ h⁻¹, and when SW-acclimated fish were exposed to hypoxia, it was not significantly different at about −10,000 nmol g⁻¹ h⁻¹ (Fig. 7B). Although the absolute unidirectional Na⁺ flux rates in SW were more than an order of magnitude higher than in fish acclimated to FW, the overall patterns of response to hypoxia were similar to those in fish acclimated to FW (Fig. 7). However, the patterns were different from those in fish acclimated to the isosmotic salinity (11 ppt), where flux increased rather than decreased during hypoxia. Note that the discrepancies in absolute values between unidirectional Na⁺ influx and efflux rates in 11 ppt- and SW-acclimated fish (Fig. 7) were likely of technical origin (see Materials and Methods), but the relative differences between normoxia and hypoxia remain comparable as they were determined by the same techniques within a salinity.

Salinity acclimation had a significant overall effect on $J_{net\ flux}^{amm}$, with elevated rates in both normoxia and hypoxia at 11 ppt relative to FW (Fig. 8). Hypoxia also had a significant overall effect, reducing rates at all salinities by 33–54%.

Gill epithelial morphology and morphometrics

The shape of ionocyte apical openings varied greatly among salinities. Fish acclimated to FW showed ionocytes that were circular, oval, triangular and roughly trapezoidal, with large exposed surfaces (Fig. 9A), compared with fish acclimated to 11 ppt and SW, which showed much smaller round and/or oval apical openings (Fig. 9B,C). The surfaces also varied between showing protruding and flat microvilli. These were smaller in fish acclimated to SW (Fig. 9C). Hypoxia-exposed fish (Fig. 9D,E,F) had PVCs which were less complex in surface, with less-developed microridges and flatter surfaces throughout. Salinity acclimation
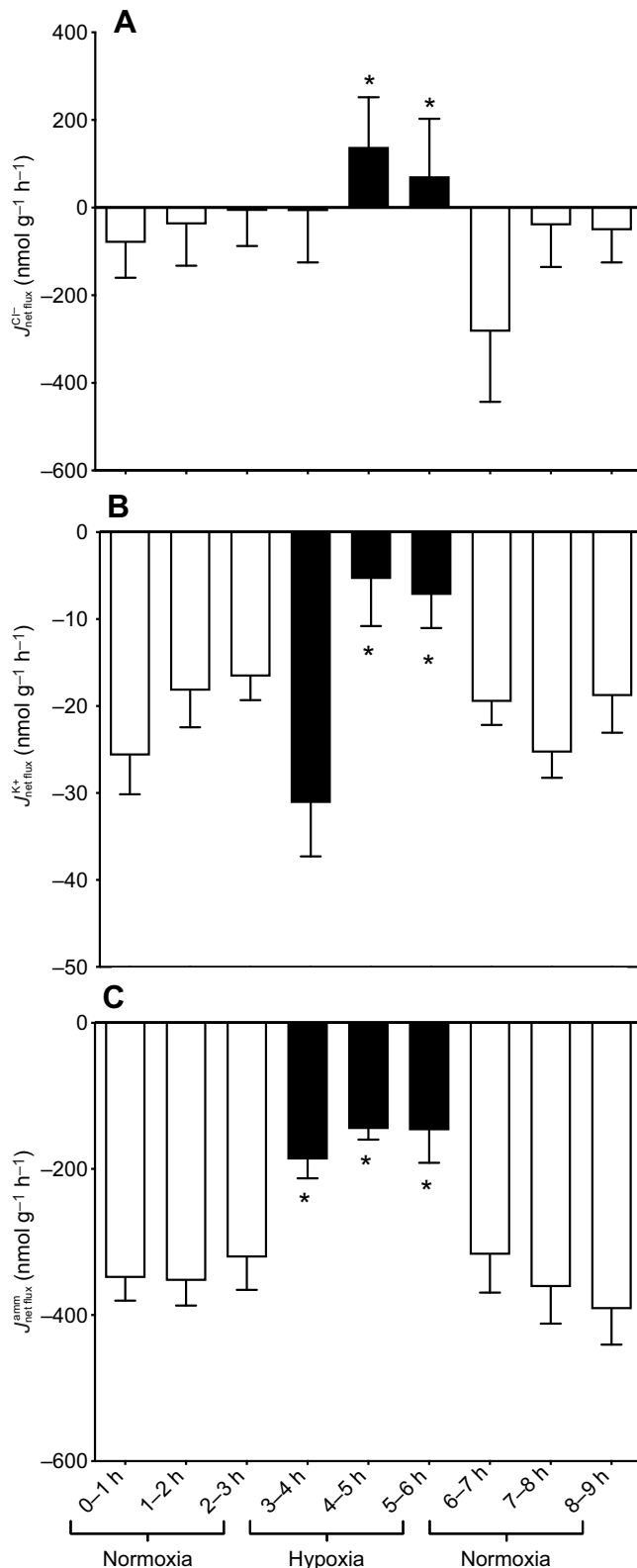
Fig. 6. Effect of hypoxia on net Cl⁻, K⁺ and ammonia flux. (A) Chloride net flux rate ($J_{net\ flux}^{Cl^-}$), (B) potassium net flux rate ($J_{net\ flux}^{K^+}$) and (C) ammonia net flux rate ($J_{net\ flux}^{amm}$) in *F. heteroclitus* acclimated to FW (0 ppt). Fish were subjected to 3 h each of normoxia, hypoxia and normoxia. Asterisks indicate significant differences from the averaged starting normoxia period (Dunnett's test). Data are means±s.e.m. (*n*=15).
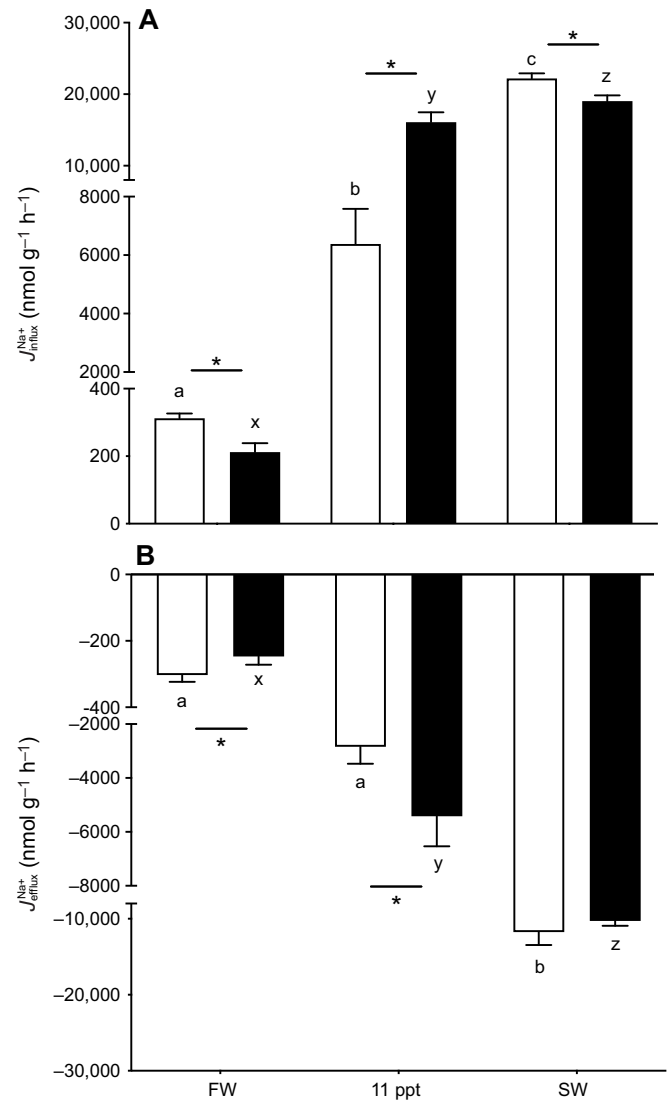

Fig. 7. Effect of salinity acclimation and hypoxia on unidirectional Na⁺ flux. (A) Unidirectional $J_{influx}^{Na^+}$ and (B) unidirectional $J_{efflux}^{Na^+}$ in *F. heteroclitus* acclimated to FW (0 ppt), 11 ppt and SW (35 ppt) in normoxia (white bars) and exposed to hypoxia (black bars). 0 ppt data are averaged data from Fig. 5. Bars sharing the same lowercase letters are not statistically different at the same oxygen level. (Two-way ANOVA *P*-values – $J_{influx}^{Na^+}$: $P_{interaction}$<0.0001, P_{oxygen}=0.0004, $P_{salinity}$<0.0001; $J_{efflux}^{Na^+}$: $P_{interaction}$=0.1059, P_{oxygen}=0.6178, $P_{salinity}$<0.0001). Asterisks indicate significant differences between normoxia and hypoxia at the same salinity (Bonferroni *post hoc* test). Data are means ±s.e.m. (*n*=15).

had a significant effect on the exposed surface area of individual ionocytes, while hypoxia exposure had no overall effect (Fig. 10A). In FW, ionocyte surface area was higher than in SW, while at 11 ppt, fish exhibited intermediate-sized ionocytes (Fig. 10A). At 11 ppt, ionocyte surface area was significantly elevated in hypoxia. Both hypoxia and salinity had significant effects on individual PVC surface area (Fig. 10B). PVC surface area was significantly higher in hypoxia at 0 and 35 ppt, while no effects of hypoxia were seen at 11 ppt (Fig. 10B). Ionocyte density was significantly affected by salinity, where FW-acclimated fish had a lower density than SW-acclimated fish. There was no significant effect of hypoxia on ionocyte density (Fig. 10C). PVC microridge density was significantly affected by hypoxia, independent of salinity
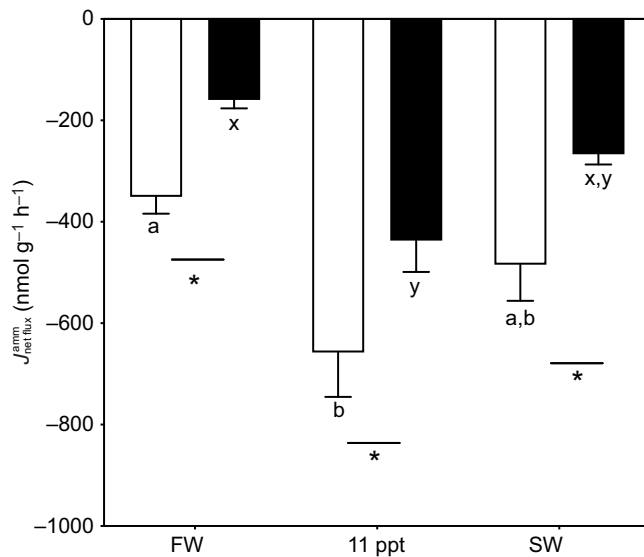
Fig. 8. Effect of salinity acclimation and hypoxia on net ammonia flux. $J^{amm}_{net\ flux}$ in *F. heteroclitus* acclimated to FW (0 ppt), 11 ppt and SW (35 ppt) in normoxia (white bars) and exposed to hypoxia (black bars). 0 ppt data are averaged data from Fig. 6C. Bars sharing the same lowercase letters are not statistically different at the same oxygen level. (Two-way ANOVA *P*-values – $J^{amm}_{net\ flux}$: $P_{interaction}=0.9560$, $P_{oxygen}<0.0001$, $P_{salinity}<0.0001$). Asterisks indicate significant differences between normoxia and hypoxia at the same salinity (Bonferroni *post hoc* test). Data are means±s.e.m. (*n*=15).

acclimation (Fig. 10D). In fish exposed to hypoxia, microridge density (intercepts per unit surface area) decreased by 42% in FW-acclimated fish, and by 23% in 11 ppt-acclimated fish (Fig. 10D). There was a significant effect of salinity on ionocyte fractional surface area, where FW-acclimated fish had higher fractional surface area than 11 ppt- or SW-acclimated fish (Fig. 10E).

DISCUSSION
Overview
Overall, our findings lend support to our hypothesis that in the killifish there is a trade-off between efficient gas exchange and ion/water balance at the gills (osmorespiratory compromise) and the nature of this trade-off is flexible, depending on environmental salinity and oxygen levels. The gas exchange components of this trade-off have been addressed in Giacomin et al. (2019), and the ion and water exchange components in the present investigation. This hypothesis led to several predictions with respect to osmoregulation. Our first prediction, that killifish would decrease gill permeability during hypoxia exposure, reducing ion and water flux in both FW and SW, was generally supported. In FW-acclimated fish, active Na^+ influx rate, gill Na^+/K^+-ATPase and NEM-sensitive ATPase activity (see Materials and Methods), ammonia, K^+ and Cl^- efflux rates, as well as diffusive water flux rates were all reduced in hypoxia. The responses of this suite of markers suggest that both transcellular and paracellular permeability were reduced during hypoxia as part of a regulated process. In SW, where Na^+ gradients are reversed, and Na^+ flux is complicated by the presence of a large exchange diffusion component, both Na^+ influx and efflux declined in accord with our prediction.

Contrary to our second prediction, in FW and SW, killifish did not show a decrease in the exposed surface area of ionocytes when exposed to hypoxia, but there was an increase in the surface area of PVCs. Nevertheless, at 11 ppt, killifish showed a significantly elevated surface area of individual ionocytes, in accord with the increased flux rates at this salinity.

Our third prediction was that because killifish acclimated to the isosmotic salinity (11 ppt) were able to prioritize gas exchange during hypoxia, as shown by Giacomin et al. (2019), they would increase permeability while exhibiting minimal disturbance of ionoregulatory homeostasis. Both unidirectional Na^+ influx and efflux rates increased as well as [³H]PEG-4000 clearance rate, in accord with our hypothesis. However, diffusive water flux rate was not altered by hypoxia. At all three salinities, plasma ions and osmolality were unaffected by hypoxia exposure, indicating that despite disturbance of ion and water flux, *F. heteroclitus* are able to maintain osmoregulatory homeostasis under hypoxia in diverse environments, via a flexible strategy with respect to the osmorespiratory compromise.

Effects of salinity and hypoxia on plasma ion homeostasis
Salinity acclimation had only a small effect on the plasma concentrations of Na^+ and Cl^- and on plasma osmolality (Fig. 1), in accord with previous studies (Wood and Marshall, 1994). In their natural habitat, *F. heteroclitus* can encounter transient as well as seasonal fluctuations in salinity; therefore, the ability to maintain ionoregulatory homeostasis is likely an adaptation for this unpredictable environment. As a result of this flexible strategy with respect to the osmorespiratory compromise, plasma ion concentration and osmolality were not significantly affected by hypoxia in killifish at any of the three salinities tested (Fig. 1), indicating a remarkable homeostatic regulation of these parameters, despite diverse changes in associated parameters such as flux rates and transport enzyme activity. In previous studies, an increase in plasma $[Na^+]$ with hypoxia was observed for two contrasting species, the hypoxia-tolerant Amazonian oscar (*Astronotus ocellatus*) (Wood et al., 2007) and the hypoxia-intolerant rainbow trout (*Oncorhynchus mykiss*) (Thomas et al., 1986). In both studies, the slight increase in plasma $[Na^+]$ was attributed to a fluid shift towards the intracellular compartment as well as a movement of Na^+ to balance the increased lactate in the plasma (Thomas et al., 1986). In our study, we observed an increase in plasma lactate concentration in response to hypoxia in FW- and 11 ppt-acclimated fish (Fig. 3B). Normoxic plasma lactate values at all salinities are comparable to those in previous studies in *F. heteroclitus* that employed similar blood-sampling techniques (Richards et al., 2008; Healy and Schulte, 2012). However, they are above resting values reported for other larger fish where blood sampling by indwelling catheters was possible (e.g. Milligan and Wood, 1986). Although blood acid–base status was not measured in the present study, Giacomin et al. (2019) reported that a comparable hypoxia exposure caused a reduction in blood pH. Therefore, it is likely that killifish are able to deal with a hypoxia-induced acidosis by employing mechanisms that are independent of the modulation of plasma ions.

Effects of salinity and hypoxia on branchial enzyme activity
A fundamental problem imposed by hypoxia exposure is the maintenance of metabolic energy balance, as a decrease in blood O_2 content directly impacts mitochondrial energy production in the form of ATP (Boutilier and St-Pierre, 2000). Hochachka et al. (1996) suggested that maintaining transmembrane electrical gradients through Na^+/K^+-ATPase is amongst the most energetically costly processes performed by a cell. Using an isolated gill perfusion preparation, Morgan and Iwama (1999) found that Na^+/K^+-ATPase and H^+-ATPase contributed to 35% of the total gill $\dot{M}_{O_2}$. Therefore, the reduction in both of these enzymes in FW-acclimated fish exposed to hypoxia (Fig. 2A,B) was in accord with the reduction of active Na^+ influx (Fig. 5A) and would have a clear benefit in terms of energy conservation. A similar rapid
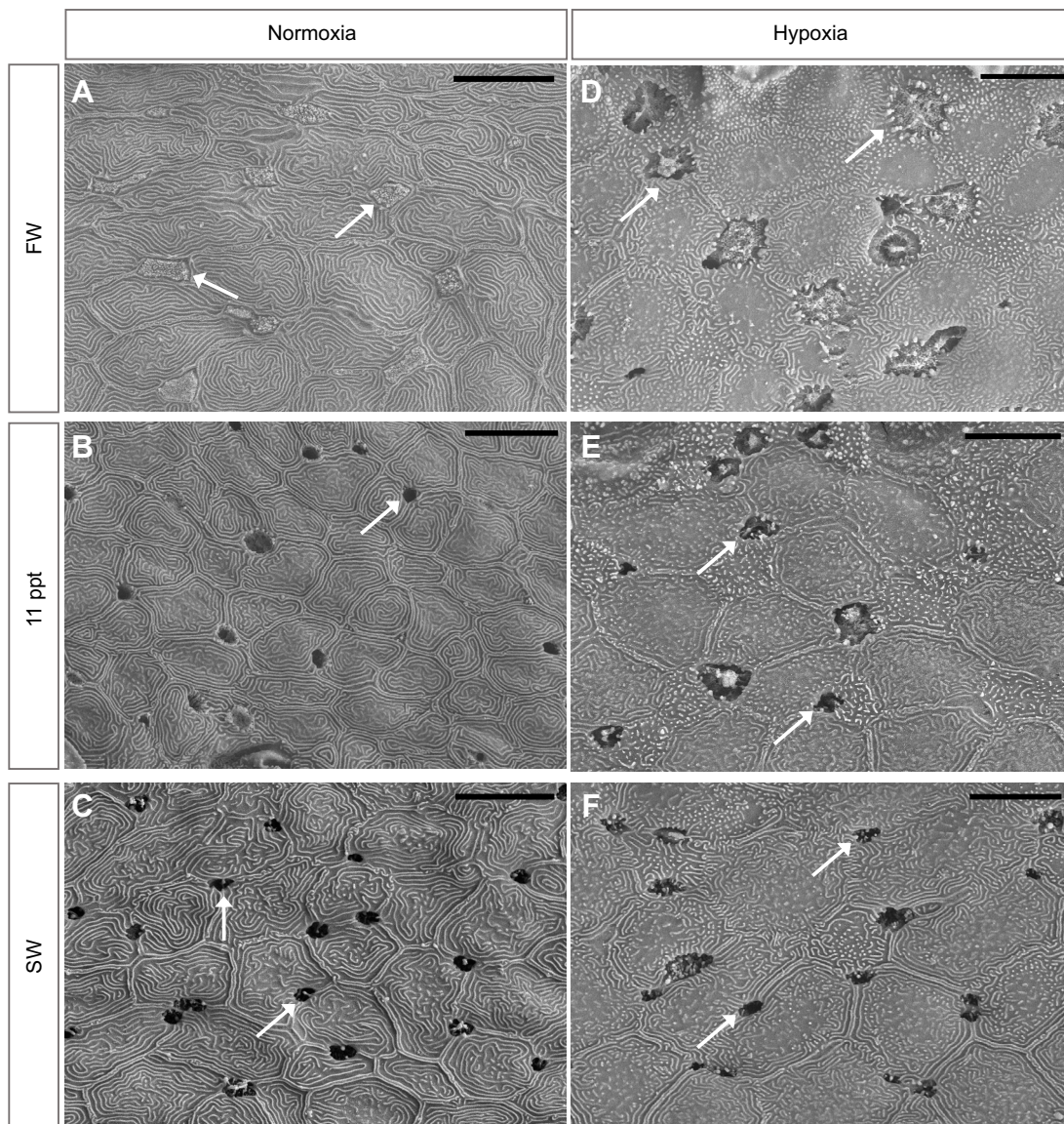
Fig. 9. Effect of salinity acclimation and hypoxia on gill epithelial morphology. Representative scanning electron microscopy images of gill filaments of *F. heteroclitus* acclimated to (A) FW (0 ppt), (B) 11 ppt and (C) SW (35 ppt) in normoxia and exposed to hypoxia for 3 h in (D) FW, (E) 11 ppt and (F) SW. White arrows indicate ionocytes. Scale bars: 10 μm.

(3–4 h) down-regulation of Na^+/K^+-ATPase activity was observed in the Amazonian oscar, where a lack of change in protein abundance raised the hypothesis that post-translational modifications may have been responsible for the reduction in enzyme activity (Richards et al., 2007; Wood et al., 2007). Notably, killifish in 11 ppt and SW did not show this response.

FW-acclimated killifish have a reduced respiratory capacity in hypoxia relative to other salinities (Giacomin et al., 2019), which could account for the different strategy that they employed in dealing with the osmorespiratory compromise. We suggest that the downregulation in enzyme activity in the FW killifish could be a reflection of the compromised respiratory ability in these animals, as a strategy to conserve energy, possibly in concert with a simultaneous downregulation of gill permeability. This way, plasma ion concentrations were maintained and whole-animal ion balance remained unaffected, in accord with our overall hypothesis of flexible responses dependent upon salinity.

Effects of salinity and hypoxia on diffusive water flux rates, paracellular permeability and drinking rates

In confirmation of our initial prediction that killifish would decrease gill ion and water permeability when exposed to hypoxia, we observed a reduction in the flux of ^3H_2O across the gills, but this effect was salinity dependent, occurring only in FW (Fig. 4A). ^3H_2O flux represents unidirectional diffusive water flux, and is approximately 100-fold larger than osmotic water flux, which is net water flux usually estimated from body mass changes and urine flow (Stevens, 1972; Isaia, 1984). Diffusive water flux is thought to occur mainly by the transcellular route (Evans 1969; Isaia, 1984), very likely through aquaporins (Evans et al., 2005), whereas osmotic water flux may occur by both paracellular and transcellular routes. Additional explanation of the significance of diffusive water flux measurements has been provided by Onukwufor and Wood (2018) and Wood et al. (2019). In general, SW teleosts have lower gill permeability to water than FW teleosts (Evans, 1969), and the water permeability of euryhaline fishes decreases with transfer to
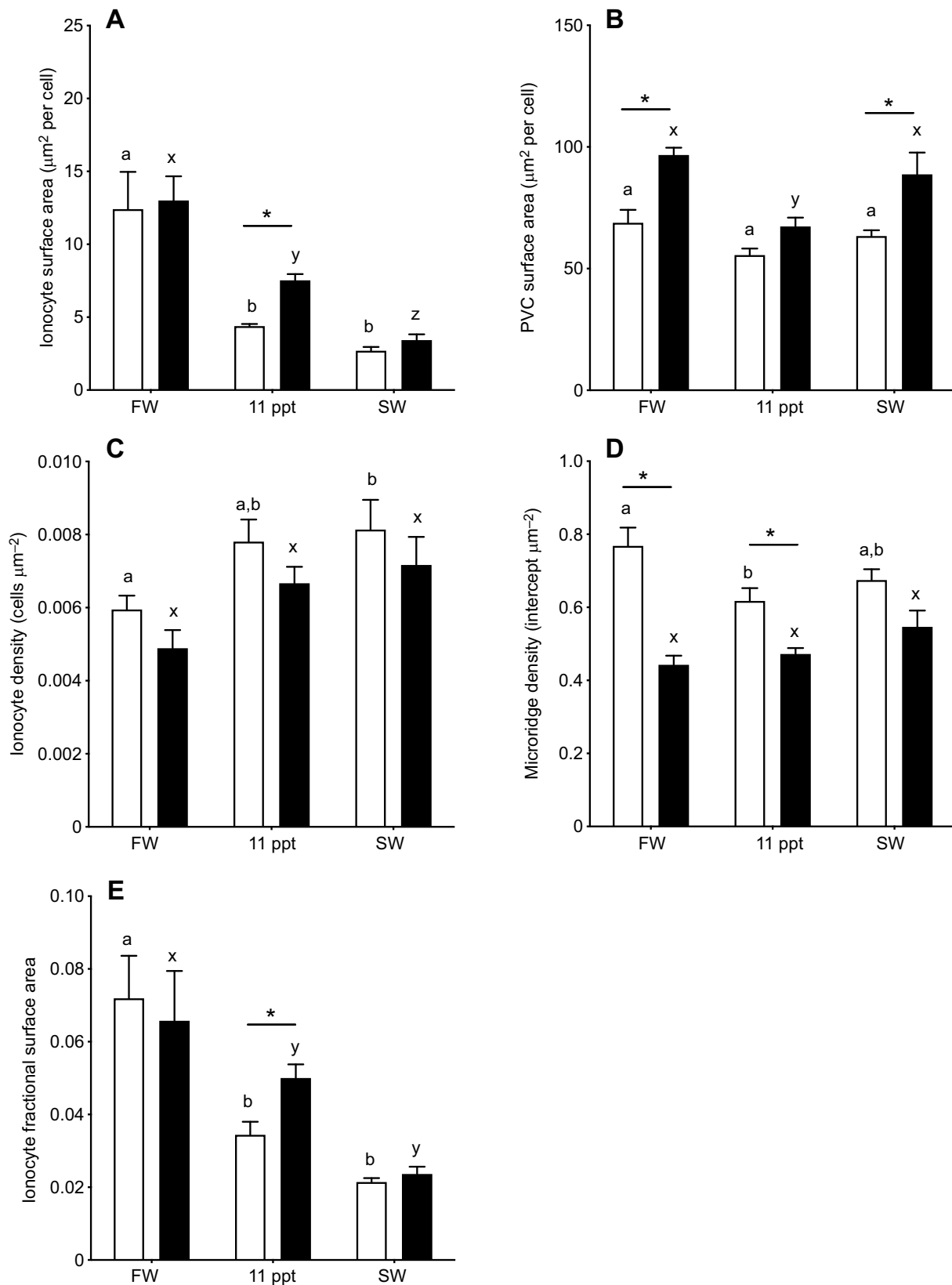
Fig. 10. Effect of salinity acclimation and hypoxia on gill epithelial morphometrics. (A) Individual ionocyte surface area, (B) pavement cell (PVC) surface area, (C) ionocyte density, (D) PVC microridge density and (E) ionocyte fractional surface area (i.e. surface area×density) in *F. heteroclitus* acclimated to FW (0 ppt), 11 ppt and SW (35 ppt) in normoxia (white bars) and exposed to hypoxia (black bars). Bars sharing the same lowercase letters are not statistically different at the same oxygen level. (Two-way ANOVA *P*-values – ionocyte surface area: $P_{interaction}$=0.5202, P_{oxygen}=0.0521, $P_{salinity}$<0.0001; PVC surface area: $P_{interaction}$=0.3175, P_{oxygen}=0.0001, $P_{salinity}$=0.0036; ionocyte density: $P_{interaction}$=0.9903, P_{oxygen}=0.0535, $P_{salinity}$=0.0050; microridge density: $P_{interaction}$=0.0275, P_{oxygen}<0.0001, $P_{salinity}$=0.1683; ionocyte fractional surface area: $P_{interaction}$=0.3634, P_{oxygen}=0.5289, $P_{salinity}$<0.0001). Asterisks indicate significant differences between normoxia and hypoxia at the same salinity (Bonferroni *post hoc* test). Data are means±s.e.m. (*n*=5).

SW (Potts and Fleming, 1970). This appears to correlate with lower expression of levels of aquaporins at higher salinities (reviewed by Cutler et al., 2007; Madsen et al., 2015; Breves et al., 2016). Our data agree with this, where in normoxia, fish that were acclimated to FW showed higher water permeability than their SW-acclimated counterparts. The decrease in diffusive water flux in FW during hypoxia but not at the other salinities may suggest the involvement of aquaporins in this response.

Our findings of reduced diffusive water flux during hypoxia in FW killifish are comparable to observations on the Amazonian oscar, which was able to reduce both diffusive and osmotic water flux during hypoxia (Wood et al., 2009), while maintaining high branchial oxygen permeability (Scott et al., 2008a). The explanation offered by these authors was that there was an adaptive reduction in transcellular permeability, due to an observed paving over of ionocytes by PVCs, in addition to channel (e.g. aquaporin) closure (Wood et al., 2009; Matey et al., 2011). Thus, we speculate that this ability to similarly downregulate gill water permeability in the FW-acclimated killifish, an effective decoupling of the classic osmorespiratory compromise, could be an adaptation to frequent variations in O_2 in their natural environments (Layman et al., 2000; Smith and Able, 2003). In contrast, gill permeability and consequently diffusive water flux rates increased markedly in both goldfish (*Carassius auratus*) and rainbow trout during exposure to moderate hypoxia – the classic trade-off of the osmorespiratory compromise response (Loretz, 1979; Onukwufor and Wood, 2018). When rainbow trout were exposed to continuing severe hypoxia, water flux rates returned to control levels, indicating some regulatory ability, perhaps involving aquaporins (Onukwufor and Wood, 2018).

[^{3}H]PEG-4000 (MW-4000) is a classic gill paracellular marker (Wood and Part, 1997) and its use in whole-animal experiments in the influx direction has been validated (Robertson and Wood, 2014). In normoxia, 11 ppt fish had lower gill paracellular permeability, in accordance with the theory that at the isosmotic salinity, the need for active Na^+ excretion would be reduced, as gradients between fish and environment are minimal, and maintenance of high paracellular permeability is unnecessary (Wood and Marshall, 1994). Paracellular permeability increased in killifish acclimated to the isosmotic medium, opposite to what was seen in fish acclimated to FW and SW (Fig. 4B). These results coupled with increased ionocyte surface area at 11 ppt (Fig. 10A) may account for the elevation in unidirectional Na^+ flux (Fig. 7A,B), suggesting that despite the maintenance of respiratory gas exchange (Giacomin et al., 2019), no compromise in ion and osmoregulation occurred.

In hypoxia, no change in [^{3}H]PEG-4000 clearance rate was seen for the Amazonian oscar, and all reductions in gill permeability during hypoxia appeared to be transcellular in nature (Wood et al., 2009), contrary to our data (Fig. 4B). Noteworthy, the absolute branchial clearance rate in the FW oscar was less than 50% of that of the killifish in FW or SW. This suggests that the oscar may more tightly regulate gill permeability in its ion-poor environment, while the FW-acclimated killifish with normally higher paracellular permeability may employ reductions in both paracellular and transcellular permeability during hypoxia as part of its flexible osmorespiratory strategy (discussed below).

Drinking rates in SW were much higher than in FW (Fig. 4C), in accord with several previous studies on *F. heteroclitus* (Potts and Evans, 1967; Scott et al., 2006; Wood et al., 2019), reflecting the fact that marine teleosts must ingest water to compensate for net osmotic water losses across the gills (Takei and Balment, 2009). SW killifish reduced drinking in hypoxia, indicating that dealing with the absorption and excretion of excess salts gained upon imbibing

SW must be an energy-demanding process. In normoxia, the stimulation of drinking in SW and its cessation in FW are both thought to be mediated by the renin–angiotensin system (Malvin et al., 1980). Possibly, the reduction of drinking in hypoxia is mediated by the same pathway; further studies on this present an interesting area for future investigations.

Effects of salinity and hypoxia on ammonia excretion

Ammonia net flux rates were inhibited by hypoxia at all three salinities (Fig. 8). In FW, $J_{\text{net flux}}^{\text{amm}}$ decreased immediately upon hypoxia exposure (Fig. 6C). It is widely accepted now that in FW fishes the majority of ammonia excretion occurs transcellularly, most likely via Rh proteins (Wright and Wood, 2009; Weihrauch et al., 2009). Therefore, the reduction in $J_{\text{net flux}}^{\text{amm}}$ is likely another indication of a reduction in transcellular permeability in response to hypoxia exposure in FW-acclimated killifish. In addition to transcellular ammonia transport, paracellular ammonia flux is also probably an important pathway in SW-acclimated fishes, given the leakier nature of junctions in SW gills (Wilkie, 1997, 2002). Giacomin et al. (2019) have shown that at low P_{O_2}, *F. heteroclitus* depresses $\dot{M}_{\text{O}_2}$ regardless of salinity acclimation, and therefore a reduction in aerobic metabolism could be an additional cause of decreased ammonia excretion.

Effects of salinity and hypoxia on unidirectional and net ionic flux rates

Fish that were acclimated to 11 ppt or SW had more than one order of magnitude higher Na^+ flux than in FW-acclimated fish (Fig. 7A), in agreement with previous studies (Motais et al., 1966; Potts and Evans, 1967; Maetz et al., 1967; Wood and Laurent, 2003; Wood, 2011). Flux in 11 ppt was 20-fold higher than that in FW, but 3.5-fold lower than that in SW (Fig. 7A). This is explained by the fact that, in contrast to FW acclimation, at higher salinities, killifish exhibit a large percentage contribution of exchange diffusion to unidirectional Na^+ flux (reviewed by Wood and Marshall, 1994). This component is proportional to external [Na^+] (Wood and Marshall, 1994), and not present in FW-acclimated animals (Patrick et al., 1997).

In our previous work (Giacomin et al., 2019), we showed that in comparison with SW- and 11 ppt-acclimated fish, FW-acclimated animals showed the greatest limitation in respiratory capacity when exposed to hypoxia. Therefore, we expected that the largest compensatory responses in order to maintain ionoregulatory balance would be seen in FW-acclimated fish. Based on the responses of the Amazonian oscar (Wood et al., 2007, 2009; De Boeck et al., 2013; Robertson et al., 2015a), we had predicted that the killifish would show a hypoxia response opposite to the classic osmorespiratory compromise in both FW and SW, decreasing overall gill permeability and ion flux. Indeed, the FW-acclimated *F. heteroclitus* showed reduced $J_{\text{influx}}^{\text{Na}^+}$ and $J_{\text{efflux}}^{\text{Na}^+}$ during hypoxia, so that no changes were seen in net Na^+ flux (Fig. 5C). Given the lack of an exchange diffusion component in the FW-acclimated killifish (Patrick et al., 1997), the very similar reductions of $J_{\text{influx}}^{\text{Na}^+}$ and $J_{\text{efflux}}^{\text{Na}^+}$ during hypoxia were probably independent of each other. The reduction in both unidirectional fluxes appear to be regulated phenomena, as they were significantly inhibited only at the second hour of exposure, remaining depressed until normoxia was restored (Fig. 5A,B). This represents an effective decoupling of the classic osmorespiratory compromise as part of the flexible strategy. Interestingly, net K^+ flux was reduced with an identical time-dependent profile (Fig. 6B). As K^+ concentrations are much higher inside cells than in blood plasma, K^+ flux is often considered a marker

of transcellular permeability (Laurén and McDonald, 1985; Wood et al., 2007, 2009; Robertson et al., 2015b), so a role for the transcellular pathway in Na+ flux reduction is implicated, as in the oscar (Wood et al., 2009). This would also be in accord with the transcellular origins of the reductions in diffusive water permeability and ammonia excretion (Fig. 6C), both discussed earlier.

FW-acclimated killifish do not take up Cl− at the gills (Patrick et al., 1997; Patrick and Wood, 1999; Wood, 2011), only at the opercular epithelium (Wood and Laurent, 2003), so the apparent reversal of net Cl− loss during hypoxia (Fig. 6A) suggests that the diffusive loss pathway at the gills for Cl− was also down-regulated. However, it should be noted that none of the positive values of Cl− flux during hypoxia (Fig. 6A) were significantly different from zero (one sample t-test). However, our results for *F. heteroclitus* point to a response different from the typical osmorespiratory compromise seen in salmonids, where ion and water flux are exacerbated when gas transfer needs to be upregulated (Wood and Randall, 1973b,c; Iftikar et al., 2010).

We earlier showed that acclimation to 35 ppt (SW) also placed constraints on respiratory performance during hypoxia, though not as severe as those at 0 ppt (FW) (Giacomin et al., 2019). At 35 ppt, fish are hypo-osmotic, so the classical osmorespiratory compromise would predict increased Na+ loading. This did not occur here – both Na+ influx and efflux rates were reduced in hypoxia by about 15%, though only the change in the former was significant, and there was no significant change in the [3H]PEG-4000 clearance rate. While the Na+ efflux component includes the active pathway through leaky paracellular junctions (Evans, 2005, 2008), it must be remembered that the major components of both unidirectional Na+ fluxes are exchange diffusion fluxes (Motais et al., 1966; Potts and Evans, 1967; Maetz et al., 1967; Wood and Marshall, 1994). Overall, these observations suggest that there was a decrease in branchial permeability during hypoxia in SW, as in FW, again providing evidence for a flexible response that is salinity dependent. Wood and Grosell (2015) have reported that acute hypoxia exposure reduced branchial transepithelial potential in *F. heteroclitus* acclimated to both 0 and 35 ppt, providing additional evidence of decreased ion flux at both salinities.

Killifish acclimated to isosmotic salinity (11 ppt) have the greatest capacity to maintain oxygen consumption in hypoxia (Giacomin et al., 2019), in accord with the idea that the osmorespiratory compromise at the isosmotic salinity is of minimal consequence. The observed increases in both Na+ influx and efflux rates coupled with the increase in the paracellular permeability likely reflected an increase in functional surface area of the gills for respiratory gas exchange. Additionally, we observed an increase in the exposure of ionocytes in hypoxia. However, the unchanged diffusive water flux rate (Fig. 4A) and the greatest lactate accumulation (Fig. 3B) at this salinity argue against our prediction. Unfortunately, no data are available for transepithelial potential in 11 ppt-acclimated fish exposed to hypoxia, which might clarify the responses seen. Perhaps there are other constraints on gill function at the isosmotic salinity of which we are currently unaware.

Salinity- and hypoxia-induced changes in gill morphology
We observed a well-established effect of salinity on ionocyte surface area (Fig. 10A), where FW-acclimated fish showed large, oval and sometimes trapezoid-shaped ionocytes (Fig. 9A), with protruding microvilli, whereas SW-acclimated fish had ionocytes with small round deep openings, called apical crypts (Fig. 9C). These salinity-specific differences in ionocyte morphology are in accordance with previous studies on FW- and SW-acclimated killifish, where

morphological differences were similarly noted (Katoh and Kaneko, 2002, 2003; Scott et al., 2008b).

Rainbow trout increase the density and exposed surface area of ionocytes shortly after hypoxia exposure (Iftikar et al., 2010; Matey et al., 2011), in accord with the typical osmorespiratory compromise (increased Na+ flux rates) shown by this species. In the Amazonian oscar, large reductions in Na+ flux rates during hypoxia were paralleled by an 80% reduction in fractional ionocyte surface area, which was largely due to covering by PVCs (Wood et al., 2009). A simultaneous increase in functional gill surface area (due to increased perfusion) and decrease in exposed ionocyte surface area was believed to maintain O2 transfer in hypoxia (Scott et al., 2008a), while concomitantly reducing gill permeability to ions. Therefore, our second prediction was that a similar mechanism would occur in hypoxia-exposed killifish. Specifically, we posited that ionocyte surface area would be reduced through a decrease in exposed ionocyte density and/or by PVCs stretching over ionocytes, thereby decreasing their exposed surface. Contrary to our prediction, hypoxia exposure in FW and SW did not change the fractional surface area of the filaments occupied by exposed ionocytes (Fig. 10E). However, individual ionocyte surface area increased in 11 ppt-acclimated fish in hypoxia (Fig. 10A). This is in accord with increased gill ion flux and paracellular permeability seen in 11 ppt-acclimated fish (discussed above). We also observed an increase in PVC surface area in FW- and SW-acclimated fish with hypoxia exposure, which could be explained by the PVCs increasing in size and spreading so as to cover up the ionocytes. This would be similar to the mechanism previously seen in oscar exposed to hypoxia (Matey et al., 2008, 2011; Wood et al., 2009). Overall, fish exposed to hypoxia show a less-complex PVC surface, where, contrary to normoxic fish, the well-defined microridge structure disappeared. The lower microridge density in hypoxia-exposed FW-acclimated fish (Fig. 10D) is in accord with this idea.

Conclusions
As the prevalence and severity of hypoxia in the world's aquatic environments increase, a comprehensive understanding of the physiological responses to hypoxia has become extremely important. Collectively, the present data elucidate the nature of the osmorespiratory compromise following acute hypoxia exposure in *F. heteroclitus* at different salinities. Salinity had a strong influence on how killifish responded to hypoxia as measured by a wide range of parameters. This was in general accord with our overall hypothesis of a trade-off between efficient gas exchange and ion/water balance at the gills that is flexible and dependent on salinity and oxygen levels. Our results show that both FW- and SW-acclimated killifish are similar to the Amazonian oscar model of response to hypoxia, inasmuch as active and passive components of gill Na+ transport were reduced, along with a decrease in water flux rates, pointing to an overall reduction in gill transcellular and paracellular permeability, particularly in FW, so that ionoregulatory homeostasis can be decoupled from the needs of respiratory gas exchange. In contrast, 11 ppt-acclimated fish increased both Na+ influx and efflux rates in hypoxia, as well as paracellular permeability, responses that follow the predictions for the classical osmorespiratory compromise. As, hypothetically, osmotic gradients are minimal at the isosmotic point, this increase in gill permeability should not be of great physiological concern. These results complement our previous study (Giacomin et al., 2019), which demonstrated that the greatest respiratory challenges for killifish during hypoxia occur in FW, and the least at the isosmotic salinity (11 ppt). Future studies should examine how these adjustments in gill permeability are achieved at cellular and molecular levels.

References

Bergmeyer, H. U. (1983). *Methods of Enzymatic Analysis*. New York: Academic Press.

Booth, J. H. (1978). The distribution of blood flow in the gills of fish: application of a new technique to rainbow trout (*Salmo gairdneri*). *J. Exp. Biol.* **73**, 119-129.

Boutilier, R. G. and St-Pierre, J. (2000). Surviving hypoxia without really dying. *Comp. Biochem. Physiol. A* **126**, 481-490. doi:10.1016/S1095-6433(00)00234-8

Breves, J. P., Inokuchi, M., Yamaguchi, Y., Seale, A. P., Hunt, B. L., Watanabe, S., Lerner, D. T., Kaneko, T. and Grau, G. E. (2016). Hormonal regulation of aquaporin 3: opposing actions of prolactin and cortisol in tilapia gill. *J. Endocrinol.* **230**, 325-337. doi:10.1530/JOE-16-0162

Cochran, R. E. and Burnett, L. E. (1996). Respiratory responses of the salt marsh animals *Fundulus heteroclitus*, *Leiostomus xanturus*, and *Palaemonetes pugio* to environmental hypoxia and hypercapnia and to the organophosphate pesticide, azinphosmethyl. *J. Exp. Mar. Bio. Ecol.* **195**, 125-144. doi:10.1016/0022-0981(95)00102-6

Cutler, C. P., Martinez, A.-S. and Cramb, G. (2007). The role of aquaporin 3 in teleost fish. *Comp. Biochem. Physiol. A* **148**, 82-91. doi:10.1016/j.cbpa.2006.09.022

De Boeck, G., Wood, C. M., Iftikar, F. I., Matey, V., Scott, G. R., Sloman, K. A., Paula da Silva, N. M., Almeida-Val, V. M. F. and Val, A. L. (2013). Interactions between hypoxia tolerance and food deprivation in Amazonian oscars, *Astronotus ocellatus*. *J. Exp. Biol.* **216**, 4590-4600. doi:10.1242/jeb.082891

Evans, D. H. (1969). Studies on the permeability to water of selected marine, freshwater and euryhaline teleosts. *J. Exp. Biol.* **50**, 689-703.

Evans, D. H. (2005). The multifunctional fish gill: dominant site of gas exchange, osmoregulation, acid-base regulation, and excretion of nitrogenous waste. *Physiol. Rev.* **85**, 97-177. doi:10.1152/physrev.00050.2003

Evans, D. H. (2008). Teleost fish osmoregulation: what have we learned since August Krogh, Homer Smith, and Ancel Keys. *Am. J. Physiol. Regul. Integr. Comp. Physiol.* **295**, R704-R713. doi:10.1152/ajpregu.90337.2008

Evans, D. H., Piermarini, P.M and Choe, K. P. (2005). The multifunctional fish gill: dominant site of gas exchange, osmoregulation, acid-base regulation, and excretion of nitrogenous waste. *Physiol. Rev.* **85**, 97-177. doi:10.1152/physrev.00050.2003

Farmer, G. J. and Beamish, F. W. H. (1969). Oxygen consumption of *Tilapia nilotica* in relation to swimming speed and salinity. *J Fish Board of Canada* **26**, 2807-2821. doi:10.1139/f69-277

Forgac, M. (1989). Structure and function of vacuolar class of ATP-driven proton pumps. *Physiol. Rev.* **69**, 765-796. doi:10.1152/physrev.1989.69.3.765

Giacomin, M., Schulte, P. M. and Wood, C. M. (2017). Differential effects of temperature on oxygen consumption and branchial fluxes of urea, ammonia, and water in the dogfish shark (*Squalus acanthias suckleyi*). *Physiol. Biochem. Zool.* **90**, 694296. doi:10.1086/694296

Giacomin, M., Bryant, H. J., Val, A. L., Schulte, P. M. and Wood, C. M. (2019). The osmorespiratory compromise: physiological responses and tolerance to hypoxia are affected by salinity acclimation in the euryhaline Atlantic killifish (*Fundulus heteroclitus*). *J. Exp. Biol.* **222**, jeb206599. doi:10.1242/jeb.206599

Gonzalez, R. J. (2011). Role of the gills: the osmorespiratory compromise. In *Encyclopedia of Fish Physiology* (ed. A. P. Farrell), pp. 1389-1394. Elsevier Inc.

Gonzalez, R. J. and McDonald, D. G. (1992). The relationship between oxygen consumption and ion loss in a freshwater fish. *J. Exp. Biol.* **163**, 317-332.

Healy, T. M. and Schulte, P. M. (2012). Thermal acclimation is not necessary to maintain a wide thermal breadth of aerobic scope in the common killifish (*Fundulus heteroclitus*). *Physiol. Biochem. Zool.* **85**, 107-119. doi:10.1086/664584

Hochachka, P. W., Buck, L. T., Doll, C. J. and Land, S. C. (1996). Unifying theory of hypoxia tolerance: molecular/metabolic defense and rescue mechanisms for surviving oxygen lack. *Proc. Natl. Acad. Sci. USA* **93**, 9493-9498. doi:10.1073/pnas.93.18.9493

Holmes, W. N. and Donaldson, E. M. (1969). The body compartments and the distribution of electrolytes. In *Fish Physiology*, vol. 1 (ed. W. S. Hoar and D. J. Randall), pp. 1-89. New York, NY: Academic Press.

Iftikar, F. I., Matey, V. and Wood, C. M. (2010). The ionoregulatory responses to hypoxia in the freshwater rainbow trout *Oncorhynchus mykiss*. *Physiol. Biochem. Zool.* **83**, 343-355. doi:10.1086/648566

Isaia, J. (1984). Water and nonelectrolyte permeation. In *Fish Physiology*, Vol. 10B (ed. W. S. Hoar and D. J. Randall), pp. 1-38. San Diego, CA: Academic Press.

Katoh, F. and Kaneko, T. (2002). Effects of environmental Ca^{2+} levels on branchial chloride cell morphology in freshwater-adapted killifish Fundulus heteroclitus. *Scan. Electron Microsc.* **68**, 347-355. doi:10.1046/j.1444-2906.2002.00432.x

Katoh, F. and Kaneko, T. (2003). Short-term transformation and long-term replacement of branchial chloride cells in killifish transferred from seawater to freshwater, revealed by morphofunctional observations and a newly established "time-differential double fluorescent staining" techniq. *J. Exp. Biol.* **206**, 4113-4123. doi:10.1242/jeb.00659

Laurén, D. J. and McDonald, D. G. (1985). Effects of copper on branchial ionoregulation in the rainbow trout, *Salmo gairdneri* Richardson. *J. Comp. Physiol. B* **155**, 635-644. doi:10.1007/BF00694455

Layman, C. A., Smith, D. E. and Herod, J. D. (2000). Seasonally varying importance of abiotic and biotic factors in marsh-pond fish communities. *Mar. Ecol. Prog. Ser.* **207**, 155-169. doi:10.3354/meps207155

Lin, H. and Randall, D. J. (1993). H^+-ATPase activity in crude homogenates of fish gill tissue: inhibitor sensitivity and environmental and hormonal regulation. *J. Exp. Biol.* **180**, 163-174.

Loretz, A. C. (1979). Water exchange across fish gills: the significance of triated-water flux measurements. *J. Exp. Biol.* **79**, 147-162.

Madsen, S. S., Engelund, M. B. and Cutler, C. P. (2015). Water transport and functional dynamics of aquaporins in osmoregulatory organs of fishes. *Biol. Bull.* **229**, 70-92. doi:10.1086/BBLv229n1p70

Maetz, J., Sawyer, W. H., Pickford, G. E. and Mayer, N. (1967). Evolution de la balance minérale du sodium chez *Fundulus heteroclitus* au cours du transfert d'eau de mer en eau douce: effets de l'hypophysectomie et de la prolactine. *Gen. Comp. Endocrinol.* **8**, 163-176. doi:10.1016/0016-6480(67)90125-6

Malvin, R. L., Schiff, D. and Eiger, S. (1980). Angiotensin and drinking rates in the euryhaline killifish. *Am. J. Physiol. Integr. Comp. Physiol.* **239**, R31-R34. doi:10.1152/ajpregu.1980.239.1.R31

Marshall, W. S. (2013). Osmoregulation in estuarine and intertidal fishes. In *Fish Physiology*, Vol. 32 (ed. S. D. McCormick, A. P. Farrell and C. J. Brauner), pp. 395-434. New York: Academic Press.

Matey, V., Richards, J. G., Wang, Y., Wood, C. M., Rogers, J., Davies, R., Murray, B. W., Chen, X.-Q., Du, J. and Brauner, C. J. (2008). The effect of hypoxia on gill morphology and ionoregulatory status in the Lake Qinghai scaleless carp, *Gymnocypris przewalskii*. *J. Exp. Biol.* **211**, 1063-1074. doi:10.1242/jeb.010181

Matey, V., Iftikar, F. I., De Boeck, G., Scott, G. R., Sloman, K. A., Almeida-Val, V. M. F., Val, A. L. and Wood, C. M. (2011). Gill morphology and acute hypoxia: responses of mitochondria-rich, pavement, and mucous cells in the Amazonian oscar (*Astronotus ocellatus*) and the rainbow trout (*Oncorhynchus mykiss*), two species with very different approaches to the osmo-respiratory compromise. *Can. J. Zool.* **89**, 307-324. doi:10.1139/z11-002

McBryan, T. L., Healy, T. M., Haakons, K. L. and Schulte, P. M. (2016). Warm acclimation improves hypoxia tolerance in *Fundulus heteroclitus*. *J. Exp. Biol.* **219**, 474-484. doi.org/10.1242/jeb.133413

McCormick, S. D. (1993). Methods for nonlethal gill biopsy and measurement of Na^+, K^+-ATPase activity. *Can. J. Fish. Aquat. Sci.* **50**, 656-658. doi:10.1139/f93-075

Milligan, C. L. and Wood, C. M. (1986). Tissue intracellular acid-base status and the fate of lactate after exhaustive exercise in the rainbow trout. *J. Exp. Biol.* **123**, 123-144.

Morgan, J. D. and Iwama, G. K. (1999). Energy cost of NaCl transport in isolated gills of cutthroat trout. *Am J. Physiol. Regul. Integr. Comp. Physiol.* **277**, R631-639. doi:10.1152/ajpregu.1999.277.3.R631

Motais, R., Romeu, F. G. and Maetz, J. (1966). Exchange diffusion effect and euryhalinity in teleosts. *J. Gen. Physiol.* **50**, 391-422. doi:10.1085/jgp.50.2.391

Nilsson, G., Löfman, C. O. and Block, M. (1995). Extensive erythrocyte deformation in fish gills observed by in vivo microscopy: apparent adaptations for enhancing oxygen uptake. *J. Exp. Biol.* **198**, 1151-1156.

Olson, K. R. (1992). Blood and extracellular fluid volume regulation: role of the renin-angiotensin system, kallikrein-kinin system, and atrial natriuretic peptides. In *Fish Physiology*, Vol. 12B (ed. W. S. Hoar, D. J. Randall and A. P. Farrell), pp. 135-254. San Diego, CA: Academic Press.

Onukwufor, J. O. and Wood, C. M. (2018). The osmorespiratory compromise in rainbow trout (*Oncorhynchus mykiss*): the effects of fish size, hypoxia, temperature and strenuous exercise on gill diffusive water fluxes and sodium net loss rates. *Comp. Biochem. Physiol. A* **219-220**, 10-18. doi:10.1016/j.cbpa.2018.02.002

Patrick, M. L. and Wood, C. M. (1999). Ion and acid-base regulation in the freshwater mummichog (*Fundulus heteroclitus*): A departure from the standard model for freshwater teleosts. *Comp. Biochem. Physiol. A* **122**, 445-456. doi:10.1016/S1095-6433(99)00030-6

Patrick, M. L., Part, P., Marshall, W. S. and Wood, C. M. (1997). Characterization of ion and acid-base transport in the fresh water adapted mummichog (*Fundulus heteroclitus*). *J. Exp. Zool.* **279**, 208-219. doi:10.1002/(SICI)1097-010X(19971015)279:3<208::AID-JEZ2>3.0.CO;2-R

Perry, S. F., Jonz, M. G. and Gilmour, K. M. (2009). Oxygen sensing and the hypoxic ventilatory response. In *Fish Physiology* (ed. A. P. Farrell, C. J. Brauner and J. G. Richards), pp. 193-253. San Diego, CA: Academic Press.

Postlethwaite, E. K. and McDonald, D. G. (1995). Mechanisms of Na$^+$ and Cl$^-$ regulation in freshwater-adapted rainbow trout (*Oncorhynchus mykiss*) during exercise and stress. *J. Exp. Biol.* **198**, 295-304.

Potts, W. T. W. and Evans, D. H. (1967). Sodium and chloride balance in the killifish *Fundulus heteroclitus*. *Biol. Bull.* **133**, 411-425. doi:10.2307/1539836

Potts, W. T. W. and Fleming, W. R. (1970). The effects of prolactin and divalent ions on the permeability to water of *Fundulus kansae*. *J. Exp. Biol.* **53**, 317-327.

Randall, D. J., Baumgarten, D. and Malyusz, M. (1972). The relationship between gas and ion transfer across the gills of fishes. *Comp. Biochem. Physiol. A* **41**, 629-637. doi:10.1016/0300-9629(72)90017-5

Richards, J. G., Wang, Y. S., Brauner, C. J., Gonzalez, R. J., Patrick, M. L., Schulte, P. M., Choppari-Gomes, A. R., Almeida-Val, V. M. and Val, A. L. (2007). Metabolic and ionoregulatory responses of the Amazonian cichlid, *Astronotus ocellatus*, to severe hypoxia. *J. Comp. Physiol. B* **177**, 361-374. doi:10.1007/s00360-006-0135-2

Richards, J. G., Sardella, B. A. and Schulte, P. M. (2008). Regulation of pyruvate dehydrogenase in the common killifish, *Fundulus heteroclitus*, during hypoxia exposure. *Am. J. Physiol. Integr. Comp. Physiol.* **295**, R979-R990. doi:10.1152/ajpregu.00192.2008

Robertson, L. M. and Wood, C. M. (2014). Measuring gill paracellular permeability with polyethylene glycol-4000 in freely swimming trout: proof of principle. *J. Exp. Biol.* **217**, 1425-1429. doi:10.1242/jeb.099879

Robertson, L. M., Kochhann, D., Bianchini, A., Matey, V., Almeida-Val, V. M. F., Val, A. L. and Wood, C. M. (2015a). Gill paracellular permeability and the osmorespiratory compromise during exercise in the hypoxia tolerant Amazonian oscar (*Astronotus ocellatus*). *J. Comp. Physiol. B* **185**, 741-754. doi:10.1007/s00360-015-0918-4

Robertson, L. M., Val, A. L., Almeida-Val, V. F. and Wood, C. M. (2015b). Ionoregulatory aspects of the osmorespiratory compromise during acute environmental hypoxia in 12 tropical and temperate teleosts. *Physiol. Biochem. Zool.* **88**, 357-370. doi:10.1086/681265

Sardella, B. A. and Brauner, C. J. (2007). The osmo-respiratory compromise in fish: the effects of physiological state and the environment. In *Fish Respiration and Environment* (ed. M. N. Fernandes, F. T. Rantin, M. L. Glass and B. G. Kapoor), pp. 147-165. Enfield, NH: Science Publishers.

Scott, G. R., Schulte, P. M. and Wood, C. M. (2006). Plasticity of osmoregulatory function in the killifish intestine: drinking rates, salt and water transport, and gene expression after freshwater transfer. *J. Exp. Biol.* **209**, 4040-4050. doi:10.1242/jeb.02462

Scott, G. R., Wood, C. M., Sloman, K. A., Iftikar, F. I., De Boeck, G., Almeida-Val, V. M. F. and Val, A. L. (2008a). Respiratory responses to progressive hypoxia in the Amazonian oscar, *Astronotus ocellatus*. *Respir. Physiol. Neurobiol.* **162**, 109-116. doi:10.1016/j.resp.2008.05.001

Scott, G. R., Baker, D. W., Schulte, P. M. and Wood, C. M. (2008b). Physiological and molecular mechanisms of osmoregulatory plasticity in killifish after seawater transfer. *J. Exp. Biol.* **211**, 2450-2459. doi:10.1242/jeb.017947

Smith, K. J. and Able, K. W. (2003). Dissolved oxygen dynamics in salt marsh pools and its potential impacts on fish assemblages. *Mar. Ecol. Prog. Ser.* **258**, 223-232. doi:10.3354/meps258223

Stevens, E. D. (1972). Change in body weight caused by handling and exercise in fish. *J. Fish Board of Canada* **29**, 202-203. doi:10.1139/f72-033

Sundin, L. and Nilsson, G. E. (1998). Endothelin redistributes blood flow through the lamellae of rainbow trout gills. *J. Comp. Physiol. B* **168**, 619-623. doi:10.1007/s003600050184

Takei, Y. and Balment, R. J. (2009). The neuroendocrine regulation of fluid intake and fluid balance. In *Fish Physiology*, Vol. 28 (ed. N. J. Bernier, G. Van Der Kraak, A. P. Farrell and C. J. Brauner), pp. 365-419. San Diego, CA: Academic Press.

Thomas, S., Fievet, B. and Motais, R. (1986). Effect of deep hypoxia on acid-base balance in trout: role of ion transfer processes. *Am. J. Physiol.* **250**, R319-R327. doi:10.1152/ajpcell.1986.250.2.C319

Tipsmark, C. K., Madsen, S. S. and Borski, R. J. (2004). Effect of salinity on expression of branchial ion transporters in striped bass (*Morone saxatilis*). *J. Exp. Zool.* **301**, 979-991. doi:10.1002/jez.a.119

Verdouw, H., van Echteld, C. J. A. and Dekkers, E. M. J. (1978). Ammonia determination based on indophenol formation with sodium salicylate. *Water Res.* **12**, 399-402. doi:10.1016/0043-1354(78)90107-0

Weihrauch, D., Wilkie, M. P. and Walsh, P. J. (2009). Ammonia and urea transporters in gills of fish and aquatic crustaceans. *J. Exp. Biol.* **212**, 1716-1730. doi:10.1242/jeb.024851

Wilkie, M. P. (1997). Mechanisms of ammonia excretion across fish gills. *Comp. Biochem. Physiol. A* **118**, 39-50. doi:10.1016/S0300-9629(96)00407-0

Wilkie, M. P. (2002). Ammonia excretion and urea handling by fish gills: Present understanding and future research challenges. *J. Exp. Zool.* **293**, 284-301. doi:10.1002/jez.10123

Wood, C. M. (2011). Rapid regulation of Na$^+$ and Cl$^-$ flux rates in killifish after acute salinity challenge. *J. Exp. Mar. Bio. Ecol.* **409**, 62-69. doi:10.1016/j.jembe.2011.08.009

Wood, C. M. and Grosell, M. (2015). Electrical aspects of the osmorespiratory compromise: TEP responses to hypoxia in the euryhaline killifish (*Fundulus heteroclitus*) in freshwater and seawater. *J. Exp. Biol.* **218**, 2152-2155. doi:10.1242/jeb.122176

Wood, C. M. and Laurent, P. (2003). Na$^+$ versus Cl$^-$ transport in the intact killifish after rapid salinity transfer. *Biochim. Biophys. Acta* **1618**, 106-119. doi:10.1016/j.bbamem.2003.08.014

Wood, C. M. and Marshall, W. S. (1994). Ion balance, acid-base regulation, and chloride cell function in the common killifish, *Fundulus heteroclitus* - a euryhaline estuarine teleost. *Estuaries* **17**, 34-52. doi:10.2307/1352333

Wood, C. M. and Part, P. (1997). Cultured branchial epithelia from freshwater fish gills. *J. Exp. Biol.* **200**, 1047-1059.

Wood, C. M. and Randall, D. J. (1973a). The influence of swimming activity on sodium balance in the rainbow trout (*Salmo gairdneri*). *J. Comp. Physiol.* **82**, 207-233. doi:10.1007/BF00694237

Wood, C. M. and Randall, D. J. (1973b). Sodium balance in the rainbow trout (*Salmo gairdneri*) during extended exercise. *J. Comp. Physiol.* **82**, 235-256. doi:10.1007/BF00694238

Wood, C. M. and Randall, D. J. (1973c). The influence of swimming activity on water balance in the rainbow trout (*Salmo gairdneri*). *J. Comp. Physiol.* **82**, 257-276. doi:10.1007/BF00694239

Wood, C. M., Kajimura, M., Sloman, K. A., Scott, G. R., Walsh, P. J., Almeida-Val, V. M. F. and Val, A. L. (2007). Rapid regulation of Na$^+$ fluxes and ammonia excretion in response to acute environmental hypoxia in the Amazonian oscar, *Astronotus ocellatus*. *Am. J. Physiol. Regul. Integr. Comp. Physiol.* **292**, R2048-R2058. doi:10.1152/ajpregu.00640.2006

Wood, C. M., Iftikar, F. I., Scott, G. R., De Boeck, G., Sloman, K. A., Matey, V., Valdez Domingos, F. X., Duarte, R. M., Almeida-Val, V. M. F. and Val, A. L. (2009). Regulation of gill transcellular permeability and renal function during acute hypoxia in the Amazonian oscar (*Astronotus ocellatus*): new angles to the osmorespiratory compromise. *J. Exp. Biol.* **212**, 1949-1964. doi:10.1242/jeb.028464

Wood, C. M., Ruhr, I. M., Schauer, K. L., Y. Wang, Mager, E. M., McDonald, D., Stanton, B. and Grosell, M. (2019). The osmorespiratory compromise in the euryhaline killifish: water regulation during hypoxia. *J. Exp. Biol.* **222**, jeb204818. doi:10.1242/jeb.204818

Wright, P. A. and Wood, C. M. (2009). A new paradigm for ammonia excretion in aquatic animals: role of Rhesus (Rh) glycoproteins. *J. Exp. Biol.* **212**, 2303-2312. doi:10.1242/jeb.023085

Zall, D. M., Fisher, D. and Garner, M. Q. (1956). Photometric determination of chlorides in water. *Anal. Chem.* **28**, 1665-1668. doi:10.1021/ac60119a009